DESIGN AND DEVELOPMENT OF SMA COATED OPTICAL FIBER SENSOR FOR CONDITION MONITORING

M.Tech Thesis

by

SHALINI SINGH

(1702103004)

Department of Mechanical Engineering

Indian Institute of Technology Indore

June 2019

DESIGN AND DEVELOPMENT OF SMA COATED OPTICAL FIBER SENSOR FOR CONDITION MONITORING

A THESIS

Submitted in partial fulfillment of the

requirements for the award of the degree

of

Master of Technology

by

Shalini Singh

Department of Mechanical Engineering

Indian Institute of Technology Indore

JUNE 2019

INDIAN INSTITUTE OF TECHNOLOGY INDORE

CANDIDATE'S DECLARATION

I hereby certify that the work which is being presented in the thesis entitled "**Design and Development of Shape Memory Alloy integrated Optical Fiber Sensor for Condition Monitoring**" in the partial fulfillment of the requirements for the award of the degree of Master of Technology in Mechanical Engineering with specialization in Production and Industrial Engineering submitted in the Discipline of Mechanical Engineering, Indian Institute of Technology Indore, is an authentic record of my own work carried out during the time period from May 2018 to June 2019 under the supervision of Dr. I.A. Palani of Discipline of Mechanical Engineering. The matter presented in this thesis has not been submitted by me for the award of any degree from any other institute.

Shalini Singh

This is to certify that the above statement made by the candidate is correct to the best of our knowledge.

Dr. I.A. Palani

Shalini Singh has successfully completed her M.Tech Oral Examination held on

Signature of Thesis Supervisor Signature of Convener, DPGC

Date: Date:

Name and signature of PSPC member 1 with date:

(**Dr. Eswara Prasad Korimilli)**

Name and signature of PSPC member 2 with date:

(Dr. Bhupesh Kumar Lad)

ACKNOWLEDGEMENTS

It gives me great pleasure to express our regards and profound gratitude to my project supervisor **Dr. I.A. Palani** (Dept. of Mechanical Engineering, IIT Indore)

for his expert guidance and unflinching support throughout project work. I am highly indebted to him for his painstaking attention towards my project and the innumerable number of improvements suggested by him, which helped me shaping my project to perfection. His competence and endurance in this regard is unquestionable. My gratitude is also extended towards PSPC members **Dr. Eswara Prasad Korimilli** and **Dr. Bhupesh Kumar Lad** for their guidance and cooperation. I would like to thank to Sophisticated Instrumentation Centre of IIT Indore for their support in providing characterization facilities and I would like to thank to all the researchers of Mechatronics and Instrumentation lab for their suggestions and help during experiments. I would gratefully acknowledge the financial aid support received from Ministry of Human Resource and Development. Special thanks to Mr. S.S.Mani Prabhu and Karthick S. for always motivating me and this work was not possible without their help. I am really grateful to **Prof. Pradeep Mathur** who provided me a helping hand by allowing me to undergo this interesting learning experience and always been a source of inspiration for me. I would like to thank to all the faculty members of the department for providing me all the required information and cooperation which played a vital role in the completion of my project in time. I would also like to thanks my parents, friends and God for their support and strong belief in me. Also I want to thank my colleagues and especially Ms. Richa Singh for providing continuous support throughout the journey.

SHALINI SINGH

ABSTRACT

The work focuses on the development of copper-based and Nickel based shape memory alloy (SMA) coated optical fiber sensor. These sensors have potential applications towards condition monitoring in different systems. The Cu-Al-Ni (82%-14%-4%) and Ni-Ti (50%-50%) SMA has been deposited on optical fiber using flash evaporation. For efficient deposition an in-situ fixture had been designed, which has a capability to induce strain and rotate the fiber to get uniform coating. The samples are prepared by varying the fixture rotational speed between 24 to 36 rpm. The deposition at 24 rpm speed has achieved maximum bending angle of 59.1º and 42º. The austenite phase transformation has confirmed at 231.15º C and 122˚C using differential scanning calorimeter. The actuation behaviour has been investigated in detail for varying load and voltage. A maximum deflection of 3.7 mm for CuAlNi coated fiber and 2.25 mm for NiTi coated fiber was achieved at 3 V against 25 mg and 35 mg load. In addition, the surface morphology, thickness measurement and thermal analysis of coated and uncoated optical fiber have been investigated in detail. Also sensing characteristics of the coated optic fiber using time vs temperature plot has been analysed using thermal camera. In this work, sensor characteristic-based parameters (response time and sensitivity) were also calculated.

LIST OF PUBLICATIONS

Journal papers

- Design and development of Cu-Al-Ni shape memory alloy coated optical fiber sensor for temperature sensing applications -Under Revision (Journal of Material Engineering and Performance)- Shalini Singh, Karthick S, Manikandan M, S. S. Mani Prabu , Suhel Khan, Brolin A, Palani I A
- Studies on Development of NiTi Integrated Optical Fiber Sensor and its Life Cycle Behaviour- Journal Under Review (Journal of Intelligent materials Systems and Structures)- Shalini Singh, Nishita Chittora , Brolin A , Palani I A
- Study of Morphological, Structural and Actuation characteristic of Cu-Al-Mn SMA coated Optic Fiber sensor- - Journal Under Review (Journal of Brazialian Society of Mechanical Science and Engineering)- Karthick S , Shalini Singh, Suhel Khan , Palani I A

Conference Papers

- Design and Development of Smart Optical Fiber Actuator for Network Switching Applications RIAM, CSIR AMPRI, 2018

- Laser polishing of Wire Arc Additive Manufactured SS 316L -AIMTDR 2018

TABLE OF CONTENTS

LIST OF FIGURES

LIST OF TABLES

ABBREVIATIONS

Abbreviation	Description
SMA	Shape Memory Alloy
POF	Plastic Optical Fiber
SEM	Scanning Electron microscope
DSC	Differential Scanning Calorimeter
TGA	Thermogravimetric Analysis

Dedicated to God

&

my Guide

Chapter 1

Introduction

Shape Memory alloys are alloys of metallic metals that return to their initial position when exposed to appropriate heat exposure. Examples of these alloys are Au-Cd, Cu-Sn, Cu-Zn-(X), Cu-Al-Ni, Ni-Al, Ni-Ti, FePt, Mn-Cu, and Fe-Mn-Si. A temperature and stress-based change happens in the crystalline structure of the material between the two distinct stages, called austenite and martensite, and thus the shape memory impact (SME) is noted. The soft stage is called the phase of martensite, and the difficult phase is called the phase of austenite. To clarify SME (shape memory effect) in action, follow a straightforward example. Consider the austenite stage of the SMA. The crystalline structure will alter to the tough stage, i.e. the martensite phase, if it is cooled below its phase transition temperature. In this work for the first time Cu-based and Ni-Ti shape memory alloy coated optic fiber sensor has been addressed for monitoring the temperature in pipelines as metal/alloy coatings excessively improve the sensing capabilities at high temperatures of the optic fiber by enhancing the sensors temperature sensitivity. Especially, Copper based Shape Memory Alloy provides improved temperature sensitivity over sensing fiber through its unique property change at forward and reverse transformations during varied heating and cooling rates. This study includes processes like Differential Scanning Calorimeter (DSC), Scanning Electron Microscopy (SEM), X-Ray Diffraction (XRD) and Thermogravimetric Analysis (TGA). For understanding its mechanisms and its one-way and two-way shape effect, a study on thermo-mechanical characterization which is named Thermal and Electrical actuation has been done. In this work, sensor characteristic-based parameters (response time and sensitivity) were also calculated.

1.1 History

Over last two decades, optical fiber sensors have attracted substantial attention and shown to be capable of monitoring various physical quantities. Fiber optic sensors have many advantages in engineering structures which include their immunity to electromagnetic and radio frequency interference, small dimensions, good resolution and accuracy as well as excellent ability to transmit signals over long distances. A recent research progress in the Plastic Optical Fiber (POF) for structural health monitoring was discussed by K S C Kuang et al[1,2]. The advantage of measuring temperature at multiple points along a single fiber is particularly interesting for the monitoring of long structures such as smart structures, pipelines, flow lines, oil wells, and coiled tubing[3,4]. Metal coating will highly protect the light transmission by reducing the attenuation level, optical non-linearity, and other deteriorations. For measuring in harsh environments, the waveguide sensor needs to be optimized and coating on the optical fiber provides improved mechanical properties at higher temperatures [4,5]. Previous literature discussed about metal coatings such as Pb, Al, Sn, PbSnAg and InBi over optic fiber based on flash evaporation technique, melt spin coating techniques etc to work as thermal sensor had been reported. However, till date shape memory alloy (SMA) coated optic fiber for temperature sensing techniques and its actuation characteristics has not been analysed in detail[5,6]. Coating of SMA over optic fiber enhances its mechanical properties by improving the microstructure and useful for fast switching response over the wide phase transformation region of SMA. Shape memory alloys are working based on the phase transformation effect activated by the application of heat. Many works have been reported using SMA thin films as an actuator[38-40]. Especially, A Ishida et al. have developed SMA based polyimide bimorph thin film actuator and studied fabrication methods with various characterization techniques and listed out its potential applications[7,8] . Copper based shape memory alloys are useful for high temperature

applications with good shape recovery, ease of fabrication and good heat conductivity [9]. Akash et al. have investigated the actuation behaviour of the copper-based shape memory alloy deposited flexible polyimide actuator developed by flash evaporation technique [10,11]. They demonstrated that film thickness and actuation parameters (voltage, current, load) affect the actuation behaviour such as displacement and shape recovery ratio. Shelykaov et al. have developed a fiber optic thermo sensitive element made of TiNiCu based shape memory alloy using melt spinning technique and measured intensity change of 10dB in the switching temperature range of 273K to 353 K [12]. J A Balta et al. [13] have developed smart composites by embedding optic fiber and SMA to act as sensor as well as an actuator. And based on the real time and simulation data, strain stabilizing feedback mechanisms have been implemented for the smart structure. K P Mohanachandra et al. have developed Nickel Titanium based SMA coated optical fiber using sputtering process to act as thermal switch, thermal sensor and thermal filter[14,15]. Akash et al have developed copper based SMA coated thin film bimorph in transformer oil temperature sensing application with higher sensing range and improved sensitivity than conventional NiTi SMA [16].

To manufacture an efficient temperature dependent, compact, lightweight and active sensor, the combination of shape memory alloy and optic fiber has been used in this work. But till date for temperature sensing applications, Cu based uniformly coated SMA over plastic optic fiber has not been reported. The developed fiber optic sensor makes it possible to measure the temperature applied to various fiber sections delimited by coupling points made of Cu-Al-Ni alloy. In this smart optical fiber sensor, the temperature range can be altered by varying the alloy and its composition, further paves way to enhance the sensing capabilities. By varying nickel content between 3-5% with appropriate Cu-Al composition have significant working range between -200^{o}C to 250^{o}C and thus here an

average of 4% nickel was selected [17,18,36,37]. Also, the selection of the Cu-Al-Ni composition for 82-14-4% will enhance the overall mechanical properties of the developed sensor [38]. Even though sputtering deposition provides control over film properties but less coating thickness, whereas flash evaporation based process has proven improved coating thickness with higher rate of deposition [19,20]. The developed samples via flash evaporation were actuated using hot plate and electrical actuation methods to analyze its capability towards sensing and bending against temperature change. Further, the quality of deposition, material and mechanical properties has been analyzed for understanding the smart optical fiber characteristics [17–20].

1.2 Shape Memory Alloy

Shape memory alloys are metallic materials that can strongly recover their initial shape when heated if they are deformed below a critical temperatur e. The shape memory effect (SME) is an apparent plastic deformation and subsequent complete recovery.

1.2.1 Shape Memory Effect

A deformed specimen that changes shape when heated characterizes the fundamental phenomenon. There is no impact of cooling on its form. Therefore, an external force is needed to re-deform the material for cyclic operation. Because shape changes occur only during heating, one-way shape memory is called the process.

A correctly processed sample can display one shape when cold in two-way shape memory, shift to a second shape when heated, and return to its initial form when cooled again, all without mechanical interference. During heating and cooling, shape change happens in two directions, although no. 3 is evolved during the shift from a high to a low temperature shape.

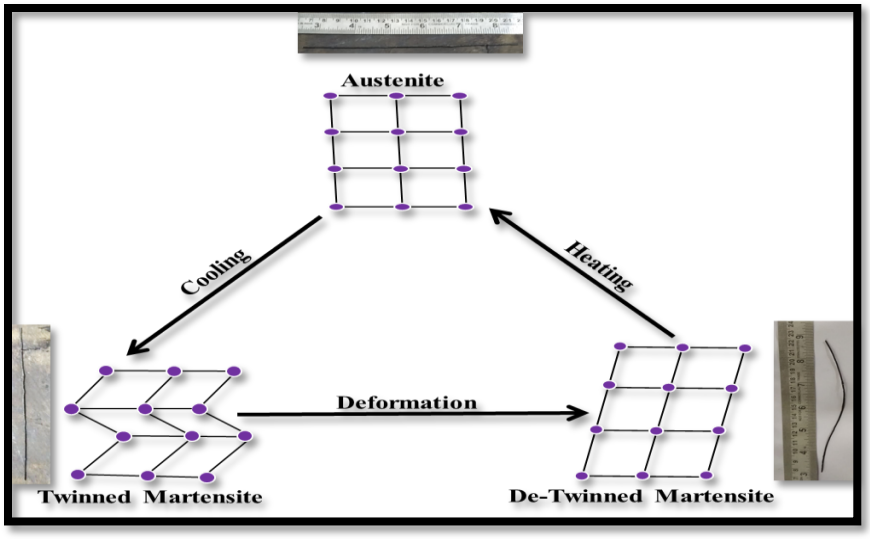

Fig. 1 Shape memory effect in SMA coated optical fiber

1.2.2 Superelasticity

A second feature is superelasticity, which is strongly linked to shape memory. If SMA material is above critical temperature, its high-temperature shape will be assumed and maintained. The material will easily soften and deform if sufficiently stressed; however, as soon as the load is removed, the material returns to its original, high-temperature shape spontaneously.

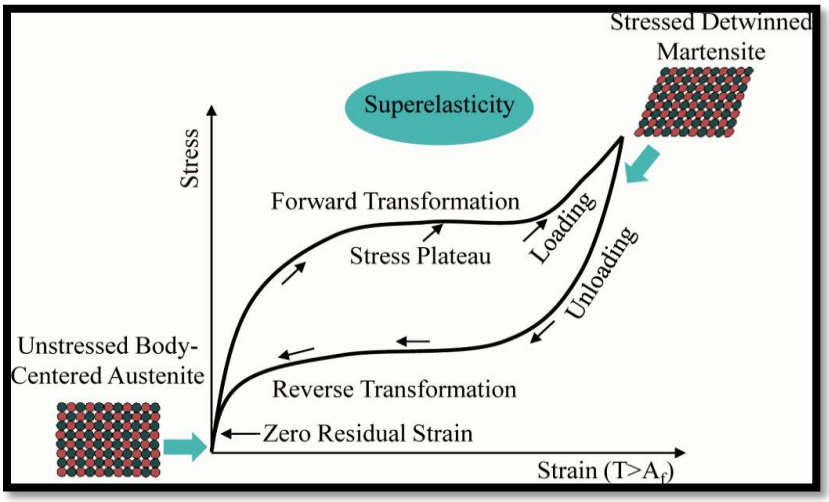

Fig. 2 Stress-strain relationship and superelasticity effect of Shape Memory Alloy

1.2.3 (CuAlNi)

The Cu based SMA alloys are much cheaper as compared to NiTi SMA Alloys. CuAlNi materials have no need to maintain sophisticated environment. It has good electrical and thermal conduction, high transformation temperature, and good thermal stability of the martensite transformation as well as large recoverable strain. Table 1 has Shown mechanical properties of CuAlNi material.

Table 1. Properties of Shape Memory Alloy (CuAlNi)

Properties	Value
Density	7.10-7.15 g/cm^3
Melting Point	1100 °C.
Resistivity	11-13 ohm-cm
Thermal Conductivity	30-43 W/cm-°C
Young 's modulus	85GPa-β Phase80GPa-martensite
Ultimate Tensile Strength	895 MPa
Shape memory strain (%maximum)	4%
Typical Yield Strength	400MPaβ Phase ,130MPa-martensite
Transformation range (^{o}C)	≤200
Transformation hysteresis(^{o}C)	15-20

1.2.4 Shape Memory Alloy (NiTi)

NiTi thin film offers many benefits including high power density, high displacement and actuating force, low operating voltage, etc. NiTi thin film is used where big force and stroke are essential, in low-duty cycles or intermittent operation, as well as in extreme settings such as room, biological and corrosive. Due to its elevated recoverable strains and big

recovery forces, NiTi is an outstanding material for use as a microactuator in MEMS devices.

Table 2: Properties of SMA (NiTi)

Properties	Value
Density Melting Point	1310 °C
Density	6.45 gm/ cm^3
Thermal Conductivity	0.1 W/cm-°C
Resistivity	76-82 ohm-cm
Ultimate Tensile Strength	754 – 960 MPa
Heat Capacity	0.077 cal/ gm-°C
Typical Elongation to Fracture	15.5%
Typical Yield Strength	100MPa-560Mpa
Latent Heat	5.78 cal/ gm
Elastic Modulus	28 – 75 GPa
Poisson's Ratio	0.3

1.3 Plastic optical fiber:

Optical fibers are used most often to transmit light between the two ends of the fiber which gives the wide range applications such as telecommunication, temperature, pressure, flowrate and conditional monitoring measurement sensor etc. The single optical fiber consists of the core and cladding structures which arrangement shown Fig.3, the fiber core has been fabricated by thin glass in which light travels. Cladding of the optical fiber will protect the fiber from moisture and damage is the buffer coating. The properties of the optical fiber are shown in Table.3.

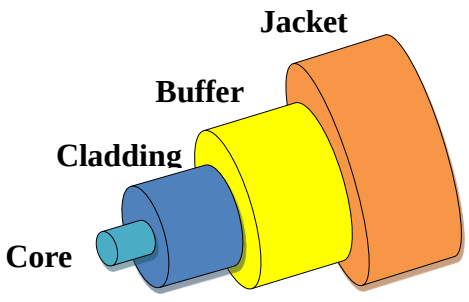

Fig. 3. Schematic of the optical fiber

Table 3. Properties of polymer optical fiber

Property	**Value**
Core refractive index	1.49
Cladding refractive index	1.46
Numerical aperture	High
Mechanical reliability	High
Bandwidth	5 MHz-km @ 650 nm
Attenuation loss	about 1 dB/m @ 650 nm

Chapter 2

Literature Review

2.1 International Status:

Nickel Titanium based SMA coated optical fiber using sputtering process to act as thermal switch, thermal sensor and thermal filter have been developed by K P Mohanachandra et al.

Shape Memory Alloy coating over optic fiber enhances its mechanical properties via microstructure improvement and useful for fast response over the wide phase transformation region of SMA. a fiber optic thermo sensitive element made of TiNiCu based shape memory alloy using melt spinning technique had been developed by Shelkyaov et al. and also demonstrated intensity change of 10dB in the switching temperature range of 273K to 353 K.

B.Sutapun et al have discussed the usage of shape memory alloys in optics application.

In a recent research progress for structural health monitoring using Plastic Optical Fiber (POF) was discussed by K S C Kuang et al.

A novel smart composites by embedding optic fiber and SMA to act as sensor as well as an actuator was developed by J A Balta et al. And based on the real time and simulation data, strain stabilizing feedback mechanisms have been implemented for the smart structure.

Metal coating will highly protect the light transmission by reducing the attenuation level, optical non-linearity, and other deteriorations. For measuring in harsh environments, the waveguide sensor needs to be optimized and coating on the optical fiber provides improved mechanical properties at higher temperatures.

Mckenzie Iain et al have experienced the importance of optic fiber sensing in european spacecraft health monitoring and its significances towards improvement in space structures health.

2.2 National Status:

For discrimination and measurement of strain and temperature, Samir K. Mondal et al. (2009) suggested a single fiber Bragg grating (FBG) sensor with two segments of distinct diameters. Using hydrofluoric acid solution, they etched the FBG to decrease the fiber diameter by factor < 1/2 to boost the sensitivity of the strain. In order to discriminate and evaluate strain and temperature, distinct changes of the Bragg wavelengths of chemically etched and nonetched gratings induced by distinct strain sensitivities were used.

B.Nanjunda Shivananju et.al. (2013) developed a finite element model to calculate the change in Bragg wavelength as a function of the thickness and refractive index of the adsorbing molecular layer by layer and compared the model with the in situ electrostatic layer assembly of weak polyelectrolytes on the EFBG slilica surface. Using the same model to arrive at a realistic estimate of the FBG sensor detection limit based on nominal measurement noise concentrations in present FBG Interrogation schemes and discovered that sufficiently thin EFBGs can provide a competitive platform for real-time measurement of moleculear interactions while the same time leveraging the elevated multiplexing capacities of fiber optics.

Kamineni Srimannarayana et al. (2008) showed that it is difficult to distinguish between the impacts of changes in strain and temperature on a single measurement of wavelength change. Fiber bragg grating simulation, long-term grating features are used to measure distinct strain-temperature reaction of mixed sensor for the concurrent measurement and discrimination of strain and temperature in C band.

Kesavean et al. (2015) stressed the use of FBG in the surveillance of structural health. Studies were performed to assess indigenous FBG senor efficiency for measuring heat strain and temperature on a steel specimen. The temperature values obtained using the indigenous FBG sensors are also compared with temperature measured from strain gauge based temperature sensor.

Anuj K Sharma et al. (2007) provided a thorough overview of Plasmon Resonance-based fiber optic sensors. A comprehensive mechanism for sensing purposes was discussed in detail with the Surface Plasmon Resonance (SPR) method. Several fresh methods and models are addressed in detail in this region. They have placed in the order of their chronological evolution the distinct methods.

A easy and compact modal interferometer was revealed by Rajan Jha et al. (2009) for refractometry apps. The unit comprises of a stub of photonic crystal fiber (PCF) that is split between conventional single-mode fibers. In the splice regions, the PCF's voids are completely collapsed, allowing the PCF core and cladding modes to be coupled and recombined. The instrument is extremely stable over time, has low temperature sensitivity, and is appropriate for 1,330–1,440 range measurement of indices. The refractive index measurement was performed by tracking the interference pattern change.

Although existing research works are available focusing on metallic coating on using fiber optics for distributed sensing there was a huge lacuna in smart material deployment in spacecraft smart health monitoring. And till date there was a lag of temperature sensing of space systems using passively powered smart techniques. Thus this provides platform to investigate the space structural monitoring with the usage of advanced functional smart material namely shape memory alloy based optic fiber sensing.

2.3 Institute / Research Group Expertise:

The proposed project's principal investigator research group has good experience of optical fiber sensors, piezoelectric, shape memory alloys, smart materials; laser based manufacturing, thin film fabrication and additive manufacturing techniques.

Akash et al have investigated the actuation behaviour of the copper-based shape memory alloy deposited flexible polyimide actuator developed by flash evaporation technique. They demonstrated that film thickness and actuation parameters (voltage, current, load) affect the actuation behaviour such as displacement and shape recovery ratio.

Akash et al have developed copper based SMA coated thin film bimorph in transformer oil temperature sensing application with higher sensing range and improved sensitivity than conventional NiTi SMA. Copper based shape memory alloys are useful for high temperature applications with good shape recovery, ease of fabrication and good heat conductivity.

S. Shiva et al. justified that the conventional route of fabrication of SMA has several limitations, like formation of stable secondary phases, fabrication of simple geometries. In this paper a simple and effective method for fabricating SMA using a laser based additive manufacturing technique is been proposed with three different compositions of Ni and Ti powders(Ni-45%Ti-55%; Ni-50%Ti-50%; Ni-55% Ti45%). These mixtures were pre-mixed using ball-milling and laser based additive manufacturing system was employed to fabricate circular rings.

Nandini Patra et al. investigated the effect of laser wavelengths and laser fluences on the size and quality of NiTi nanoparticles generated by the Nd: YAG laser ablation technique underwater solid state. The tests were conducted on Ni55 percent–Ti45 percent sheet to synthesize NiTi nano-

particles at three distinct wavelengths (1064 nm, 532 nm and 355 nm) with distinct laser fluences ranging from 20 to 40 J / cm2.

K. Akash et al. experimented the life cycle and thermomechanical behaviour for quaternary CuAlNiMn alloy, developed through thermal evaporation technique on flexible Kapton polyimide substrate. The thermomechanical behaviour was studied by actuating the composite film through Joule heating under different loads of 30 mg, 45 mg and 60 mg. Parameters such as voltage and frequency were varied to analyse the actuation properties. The composite bimorph required less than 2 V to displace 4 mm under 60 mg load. The life of eight samples was recorded for more than 20,000 cycles, and the reliability of the film showed good result.

S. Shiva et al. recorded the behavior of alloyed shape memory (SMA) laser additive production (LAM) constructions using three TiNiCu premixed compositions (Ti50Ni(50−x)Cux(x= 5, 15 and 25)). Using an additive manufacturing scheme based on 2 kW laser fiber. The processing parameters have been optimized for defect-free deposition; the optimized parameters have subsequently been used for structure LAM.

K. A two-way Cu-Al-Ni / Polyimide shape memory alloy bi-morph was created by Akash et al. without any post processing. With shape memory effect, the forward stroke was accomplished and the return stroke was due to the impact of flexible polyimide substratum. They developed a custom made setup with electrical heating to investigate the life cycle of the bi-morph at different voltages, ranging from 2 V to 3 V. The austenite transformation temperatures of the bi-morph, was found to be As= 215 ◦ C and Af= 240 ◦ C.

S. Shiva et al. developed a substitute using Cu with Ni upto 15 wt% to 30 wt% to possess shape memory properties. In this paper an investigation

was carried out with a combination of Ti50% Ni25% Cu25% alloy formation and is represented as NiTiCu25.

Tameshwar Nath et al. researched the loss of actuation by designing and analyzing the spring of shape memory alloy actuated by warm water. Intelligent materials display unique characteristics that make them a preferred option in many engineering fields for industrial applications. They demonstrated that a Ni-Ti piece's serviceable characteristics can be enhanced by changing the source of energy. The temperature reaches 70 ° C-90 ° C with warm water actuation, the spring is fully compressed for the first few cycles followed by loss of actuation..

Friction Stir Welding (FSW) has effectively entered NiTi with S.S Mani Prabu et al. Without formation of detrimental stages, the weld showed important grain refinement. The yield strength of the weld joint increased by 17% as compared to the base metal without substantial change in shape memory behaviour.

S. Shiva et al. proposed that Ni-Ti shape memory alloys can be accomplished by annealing for micro-electro-mechanical systems manufactured using laser additive manufacturing and requiring homogeneous microstructure for predictive design and manufacturing of micro-electro-mechanical systems. Research has been carried out on laser annealing of laser additive-manufactured Ni-Ti constructions through numerical simulation and experimental research using a pulsed green laser. Rite anything you want. To paraphrase it, click the Quill It button on the right.

Pradeep et al have developed a reliability model of smart material using a GLL-Weibull analysis. For estimating the life prediction of SMA spring during thermomechanical fatigue integrated study of GLL Weibull distribution within a Bayesian framework was proposed. Here an SMA

actuation study was analyzed whereas sensing was proposed in our work for the first time.

Nandini Patra et al have generated NiTi nanoparticle using liquid assisted laser ablation and investigated the reaction by varying with laser wavelength and analysed the effect of the change in speed of the rotating Nitinol target.

Reena Disawal et al created the life cycle analysis of an SMA spring using the interferometric technique of Talbot and evaluated the displacement dri ft, which sets in owing to the functional fatigue produced by its repeated u se.

2.4 Research Gap Identification:

Previous literature discussed about metal coatings such as Cu, Ni, Pb, Al, Sn, PbSnAg and InBi over optic fiber based on physical evaporation evaporation technique, melt spin coating techniques etc to work as thermal sensor had been reported. But, till date shape memory alloy (SMA) especially Cu-based coated optic fiber for temperature sensing techniques and its actuation and lifecycle characteristics has not been analysed in detail both national and international level. Thus recovering the waste heat from space system for active sensing using SMA is a advanced concept where less power consumption, and compact size of optic fiber also plays a wide role in novel sensing and monitoring health of space structures.

Chapter 3

Experimental Set-up

3.1 Experimental Procedure:

3.1.1 For CuAlNi coated fiber

Copper, Aluminum and Nickel wires [Cu-Al-Ni (Cu, 14Al wt.%, 4Ni wt.%) (Sigma Aldrich, purity 99.9%) has been measured using precision balance (sum of 1 g) and used for deposition by placing on tungsten boat in the evaporation chamber and its properties are already shown in the Table 1 [21]. Flash evaporation deposition technique has been used for developing Cu-Al-Ni thin film on plastic optical fiber with high vacuum condition (5x10-5 mbar). The flash evaporation schematic is shown in Fig. 4. The optical fiber (1mm diameter, 0.5 mm core diameter and length 210 mm) was mounted in an in-situ rotatable fixture Fig. 5, which will assist to obtain uniform deposition of the entire surface area. Before loading in the chamber the optical fiber samples are pre-strained 5.55% using mechanical loading[22]. The plastic optical fiber consists of core and cladding structure construction and its properties are shown in Table 3 [23].

Three rotating speed were selected (24, 30 and 36 rpm) for deposition of SMA over optical fiber. During deposition, room temperature was maintained, and 40 A current has been used for evaporating the Cu-Al-Ni pellets from tungsten boat. The evaporated material was deposited on the bare optical fiber. Due to thermal stress the removed coated optical fiber was appeared like bended into semicircular shape. To study the morphological and structural properties, the sample has been characterized by using scanning electron microscope (SEM) and X-Ray diffractometer (XRD) respectively. To understand the thermal characteristics, different thermal analysis such as Differential Scanning Calorimetery (DSC) and Thermogravimetric Analysis (TGA) has been

used. The heating and cooling rate were maintained at 10 °C/min for 15 mg sample.

To probe the suitability of utilizing the optical fiber in MEMS application, a set-up based on Joule heating (electrical actuation) was used for the analysis of the sensing and bending abilities as shown in Fig. 6. The setup consists of laser displacement sensor, computer, data acquisition system (Agilent DAQ 34790A), thermo optical actuator and programmable power supply (RIGOL DP1308A by LXI). For this actuation analysis, three different loads and voltages were used.

Table 4: Experimental Parameters for (CuAlNi)

SR. NO.	WEIGHT (mg)	SPEED (rpm)	PRESSURE (mbar)	CURRENT (Amp)	ACTUATION
1	1000	20 rpm	5*(10^-5)	40	No
2	1000	24 rpm	5*(10^-5)	40	Yes (good in cooling and good in heating)
3	1000	30 rpm	5*(10^-5)	40	Yes(slow cooling)
4	1000	46 rpm	5*(10^-5)	40	Yes (slow cooling)

- Target Material – CuAlNi
- Material Composition – 82%-Cu,14%-Al,4%-Ni
- Substrate Heater Temperature – 32 °C
- Substrate - Optical fiber
- Substrate Specifications - 1 mm Diameter(0.5mm Core), length = 22cm
- Strain =5.75%-7%

3.1.2 For NiTi coated fiber

Wires of Nickel and Titanium (50% Ni and 50% Ti) has been measured with help of the precision balance and was used for deposition. From the NiTi phase diagram, equiatomic composition of Nickel and Titanium has been selected for better transformation. The NiTi sample has been used for deposition by placing on a tungsten boat in the evaporation chamber and its properties are shown in the Table 2[21]. Flash evaporation based physical evaporation deposition method has been used for developing NiTi thin film on plastic optical fiber with high vacuum condition (5x10-5 mbar) and at room temperature. The polymer optic fiber (1mm diameter, 0.5 mm core diameter and length 200 mm) was mounted in an in-situ rotatable fixture Fig. 5, which will assist to obtain uniform deposition of the entire circumference of the fiber. The optical fiber samples are pre-strained 5% using mechanical loading (Abdi et al., 2008). A current of 80 A has been used for evaporating the NiTi samples from a tungsten boat. Using a SEM and XRD, the morphological and structural properties of the sample has been characterized, respectively. Phase transformation temperature and thermal characteristics has been analyzed using DSC and TGA.

To explore the suitability of optic fiber in MEMS application, a electrical Joule heating setup was made for the analysis of displacement and bending abilities as shown in the schematic diagram in Fig. 7. The setup consists of a laser displacement sensor, data acquisition system, Arduino-relay circuit, thermo-optical actuator, and a programmable power supply. The arduino relay circuit acts as a switch which alternates between heating and cooling of the SMA embedded in the optical fiber for a duty cycle of 15 seconds. For this actuation analysis three different loads and voltages were used.

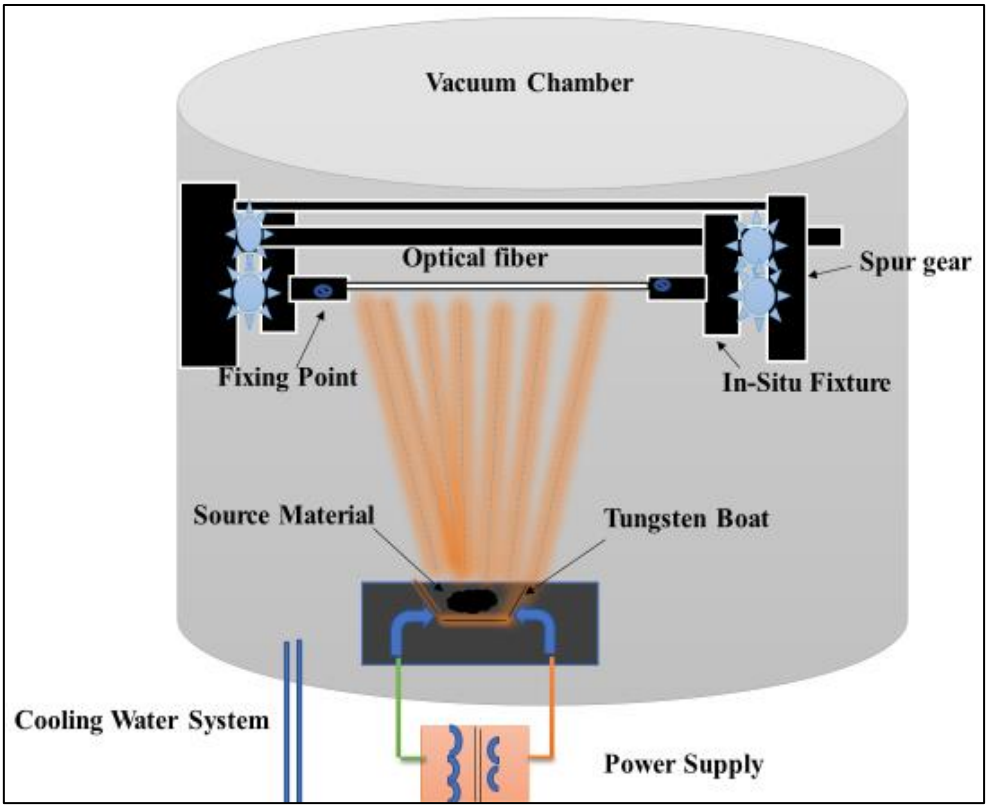

Fig. 4 Schematic of flash evaporation deposition setup

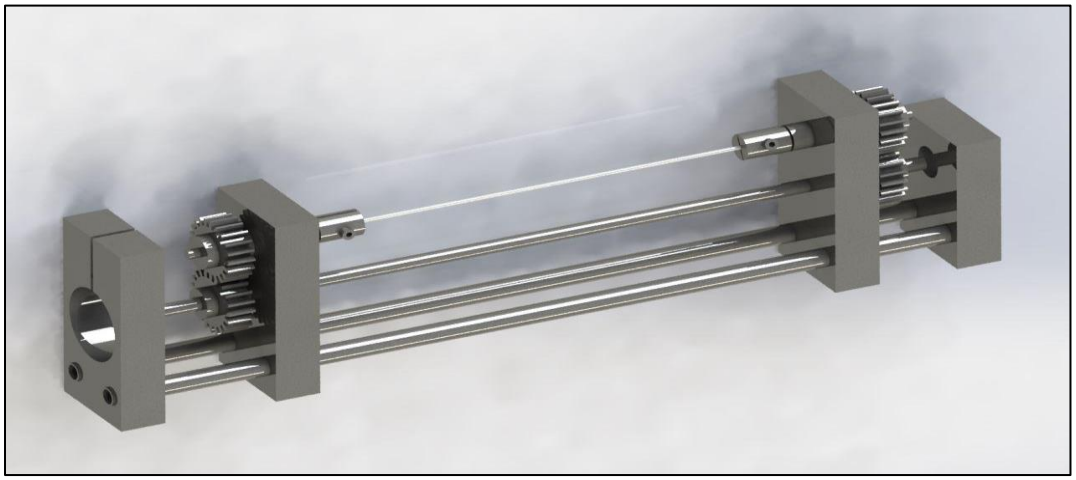

Fig. 5 Optical Fiber In-Situ Fixture setup

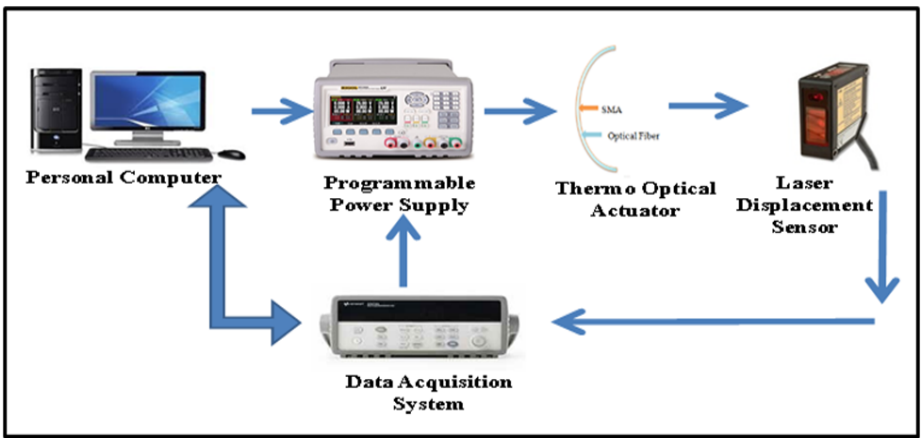

Fig. 6 Schematic of electrical actuation setup

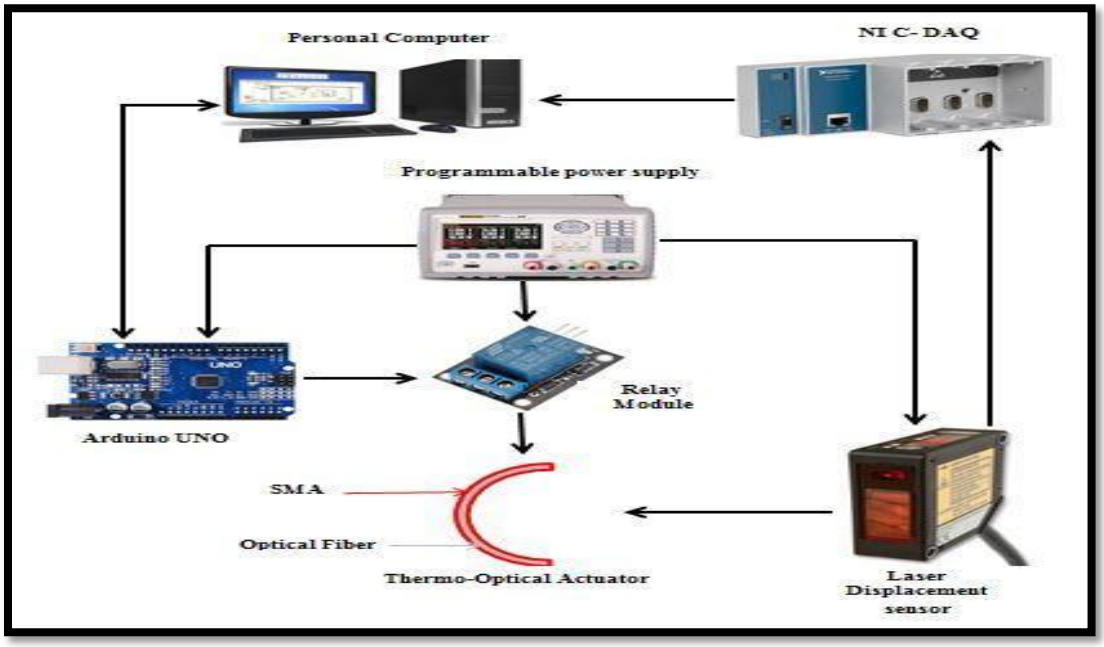

Fig. 7 Block diagram of life cycle analysis

Chapter 4

Structral and Morphological analysis of SMA coated Fiber

4.1 Optical Microscopy

An optical microscope has been used to analyze the Cu-Al-Ni coated optical fiber thickness and film surface. The schematic of SMA coated optical fiber is shown in the Fig. 8(a) and the
photograph of bare and coated optical fiber is shown in Fig. 8(b). The thin film surface of the coated optical fiber has exhibited uniformity and layered structure grown by flash evaporation deposition as shown in Fig. 8(c). The cross sectional of the bare and coated optical fiber is shown in Fig. 8(d) and (e). The coating thickness and interface sharpness was controlled by rotational speed during deposition (Ref 24). The thickness of SMA coating over the optical fiber has been evaluated by optical microscope which is ≈12.96 micron (Fig. 8e).

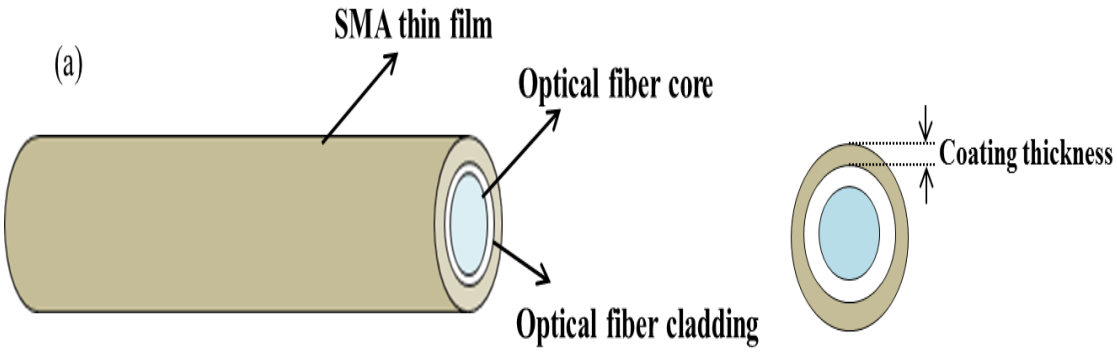

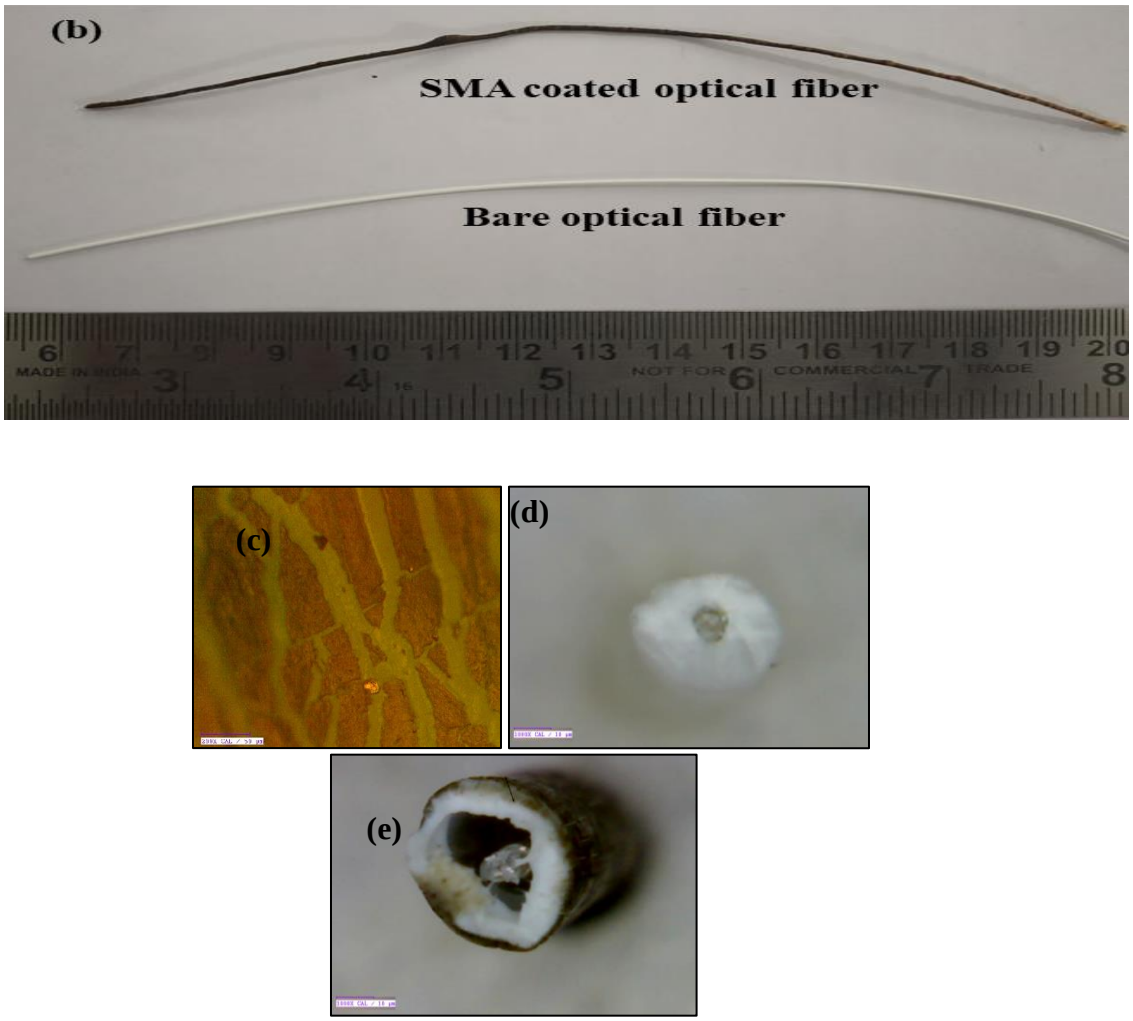

Fig. 8 (a) Schematic of SMA coated optical fiber (b) Photographs of bare and SMA coated optical fiber (c) microscopic images of Cu-Al-Ni coated fiber, (d) cross sectional view of the bare optical fiber and (e) cross sectional view of the SMA coated optical fiber

4.2 Morphology and Elemental Analysis

4.2.1 For CuAlNi coated fiber

Fig. 9(a) and (b) shows the surface morphology of Cu-Al-Ni coated fiber and composition analyzed using scanning electron microscope and Energy Dispersive Spectroscopy (EDS) respectively. SMA deposited at varying rotational speed, displayed similar morphological and structural information. All the images of the developed films displayed the texture patterns, which were probably martensitic structures. The image depicted

smooth uniform morphology with very few cracks and pores implying that Cu-Al-Ni coating was successfully deposited on plastic optical fiber. The grain size as measured has found to be approximately ranging from 50 nm to 150 nm, which is very less than the developed alloy through the conventional process. Also, precipitates were found at different places as seen from SEM images. The layered morphological structure could have formed due to difference in evaporation temperature of copper, aluminum and nickel wires, used for deposition [25]. The EDS analysis was performed at different five locations. The average value has displayed minor deviation from the composition of Cu, Al, and Ni measured prior to the deposition as shown in Table 5.

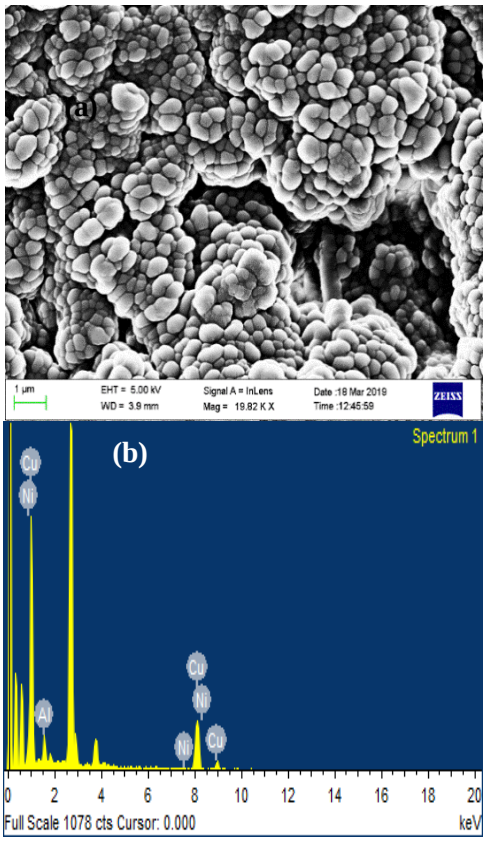

Fig. 9 SMA coated optical fiber **(**a) surface morphology and (b) EDX result

Table 5 EDS report of Cu-Al-Ni SMA coated fiber

Elements	Weight%
Al	14.20

Ni	03.00
Cu	82.80

4.2.2 For NiTi coated fiber

The samples of the fiber coated with NiTi were characterized using SEM to examine the morphology of the developed coating. Even though the coating, on a broad view appeared to be rough and uneven throughout but the surface, as observed is layered. This is due to the dissimilar evaporating temperatures of Ni and Ti which are taken in the form of wires due to which they get coated layer by layer over the fiber and thus the surface appears layered [25]. The SEM image obtained, shows that the film exhibits a typical amorphous microstructure. Average Grain size is found out to be approximately 330 nm. Also, the micrographs of the cross sections illustrate the presence of columnar grains. Precipitates of nickel are observed throughout the surface. Electron Dispersive Spectroscopy (EDS) is carried out to determine the compositions of the coatings of NiTi over the optical fiber. This was done at 10 different points and then the average is considered for determination. The recorded compositions of the coatings in terms of Ni and Ti after deposition are 58.2 and 42.8wt% respectively. Minor deviations from the original composition are observed because of difference in vapour pressure of source material [26] during deposition. A slight increase in the amount of Ni is evident from the measurements while a decrease in the amount of Ti is recorded.

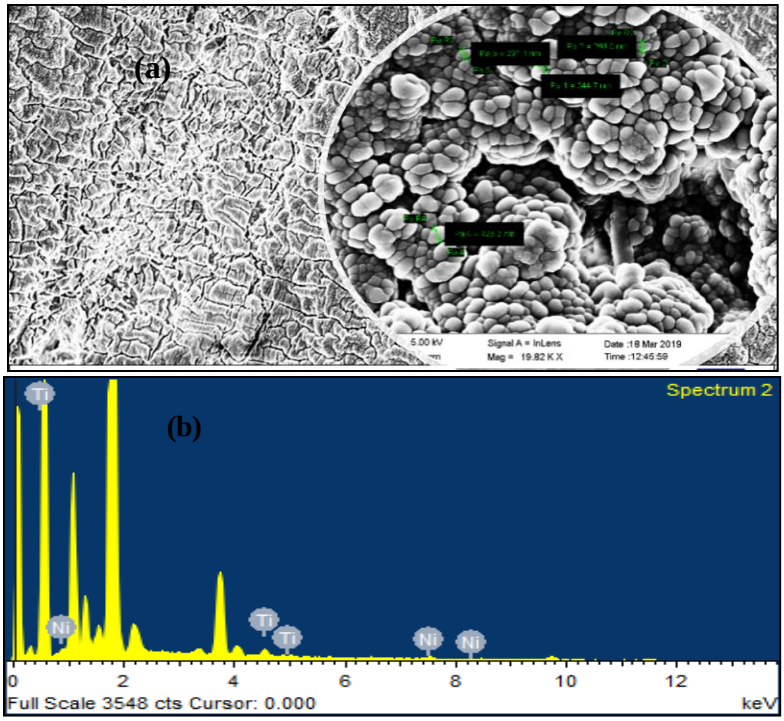

Fig. 10 NiTi coated optical fiber (a) surface morphology and (b) EDX result

Table 6. EDS Composition for NiTi

Elements	Weight%
Ni	65.2
Ti	35.8

4.3 Atomic Force Microscopy

The substrate orientation and cladding interface layer have a markable influence on the surface morphology of deposited CuAlNi-based films and results in a more homogeneous island distribution. The RMS surface roughness is closely related to the mean island size and island distribution. For homogeneous island distribution, the larger the mean island size, the higher the RMS surface roughness. The inhomogeneous island distribution always results in a higher RMS value. The Flash Evaporation based deposition technique has been used to deposit CuAlNi shape memory alloy over the glass substrate. To investigate the as deposited thin film quality, AFM is used. Because, the AFM techniques is the adequate method to study the processing quality and verification of thin films, nanostructures dimension, substrate orientation and roughness. Therefore, In

order to corelate and confirm the surface morphology observed using FE-SEM, an AFM experiment has been conducted. The corresponding surface structure is clearly described using AFM micrograph in Fig 11. In present case an AFM characterization has been performed in non -contact mode. Formations of nano-sized grains were confirmed by analysing the micrographs presented in Fig11. The RMS roughness of the CuAlNi thin films was found to be 0.002 micron. This ensures the smooth coating of alloy material over the optic fiber's cladded surface. Fig. 11 shows the surface morphology of CuAlNi thin films deposited at room temperature on a glass substrate. From the observation, the film contains nearly globular islands with grooved boundaries. Because sphere has the smallest surface area relative to other types, therefore the smallest surface energy was observed. The film positioned on a glass slide substratum is made up of large groups of islands up to 1000 nm in diameter. Each group of islands is comprised of several smaller islands with a diameter of about 175–250 nm. The CuAlNi coated thin film's RMS surface roughness is about 2.15 nm in an region of 1x1 μm2. With regards to the different RMS values in the deposited films, they are possibly related to the mean island size and island group boundaries in the examined area.

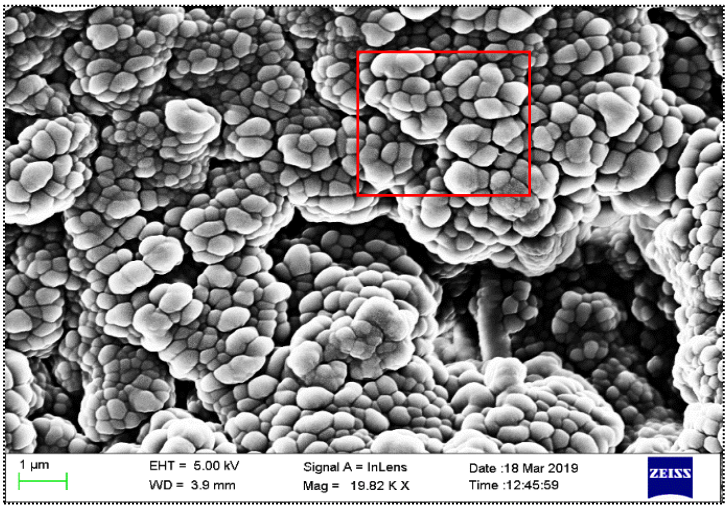

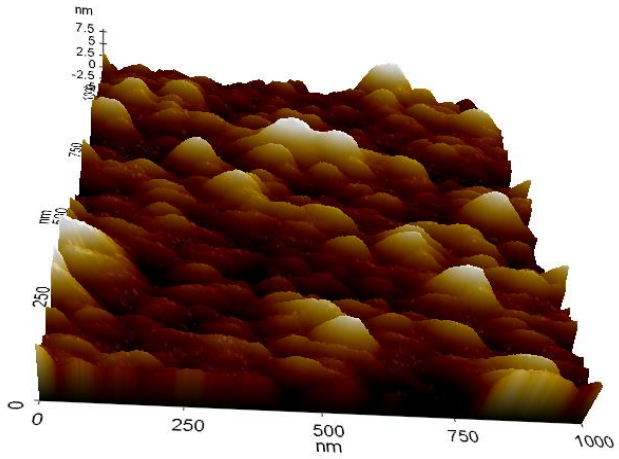

Fig. 11 SEM and AFM image of the CuAlNi Thin Film

4.4 X-Ray diffraction:

4.4.1 For CuAlNi coated fiber

Fig. 12 shows the X-ray diffraction pattern for Cu-Al-Ni coated optical fibers which has been coated at different speed of in-situ fixture. It is observed that the highest peak for all coated sample corresponds to martensitic phase at 44.280 which shows the presence of crystalline β_1' (128) (ICSD pattern, card no: (01-077-8149)) along with γ_1'martensite belonging to monoclinic structure [27]. The crystallite size for this peak was 5.14 nm, which has been determined from Scherer equation [28] . The other minor peaks displayed different crystal lattices at 2θ corresponding to (29.4°, 64.7° and 82.07°) indexed as (101), (018), (200) and (0217) planes respectively. It shows trigonal lattice structure and $Al_{17}Cu_4Ni$ compound at 24.6° and at 29.4° it indicates cubic lattice structure with the formation of $Cu_9Al_4Ni_{0.5}$ compound and for both 64.7° and 82.07 ° it shows trigonal lattice structure but compound is different. At 64.7°, it shows $Al_{20.88}$ $Cu_{12.14}$ $Ni_{3.04}$ and at 82.04° $Al_{17}Cu_4Ni$ compound is formed. But in case of coating at high speed (36 rpm) two more peaks is coming at 35.29°, 52.42° and 54.47°, indexed as (0111), (205) and (208) belonging to trigonal lattice structure. The compound formed at 35.29 is $Al_{20.88}$ $Cu_{12.14}$ $Ni_{3.04}$ and $Al_{17}Cu_4Ni$ formed at remaining two peaks. The coated fiber at

36 rpm has more peaks because of less coating thickness at higher speed. In case of bare fiber there are two minor peaks at 24.38° and 34.7° belonging to (111) and (002) miller indices [28].

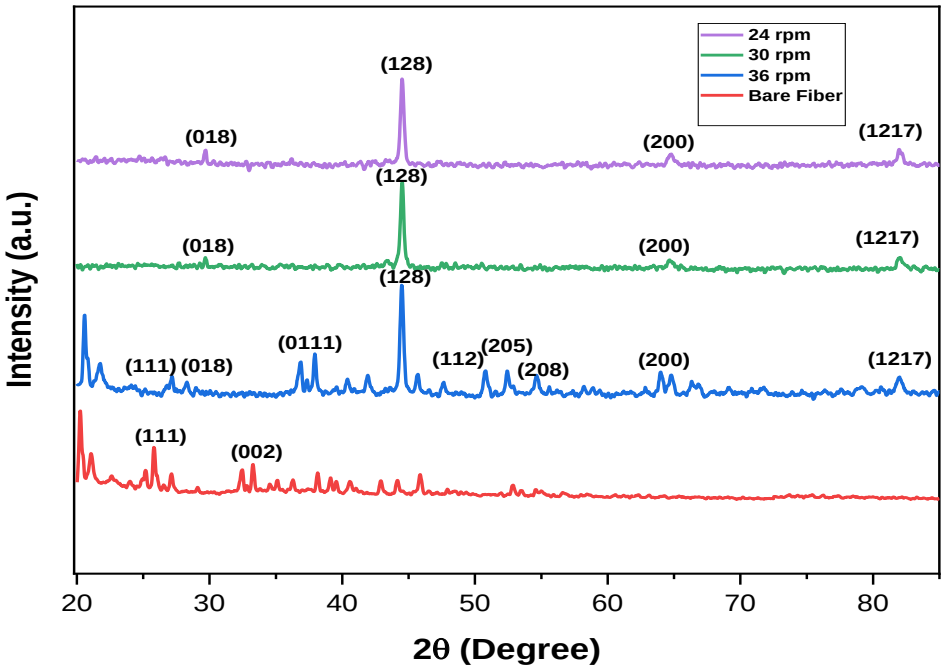

Fig. 12 XRD graph of bare fiber and Cu-Al-Ni coated optical fibers

4.4.2 For NiTi coated fiber

The XRD pattern of NiTi coated optical fiber is obtained as shown in Fig. 13. There are various intermetallic phases identified in the coating, martensitic NiTi, austenitic NiTi, NiTi2 and Ni3Ti. The major, high intensity martensitic peak is observed at 2θ = 44.38° along the plane (0 2 0) which reveals the presence of monoclinic phase there. The film is quite well crystallized during the deposition process, which may be seen from the plot, as the peak is sharp. At 2θ = 64.7° on the plane (0 1 23) and 2θ = 81.81° at (9 3 1), rhombohedral and cubic lattice structures are observed, respectively. However, these peaks are somewhat broader in comparison to the major peak which shows some amorphous character in them. Various other minor peaks are also observed between 30o to 85o. Thus, the fiber coated with NiTi, in the martensitic phase, exhibits a monoclinic structure, rhombohedral structure in R phase and cubic structure in the austenite phase. The two way shape memory effect is amplified in NiTi

due to the presence of R phase [44].This happened because of Ni percipitates.

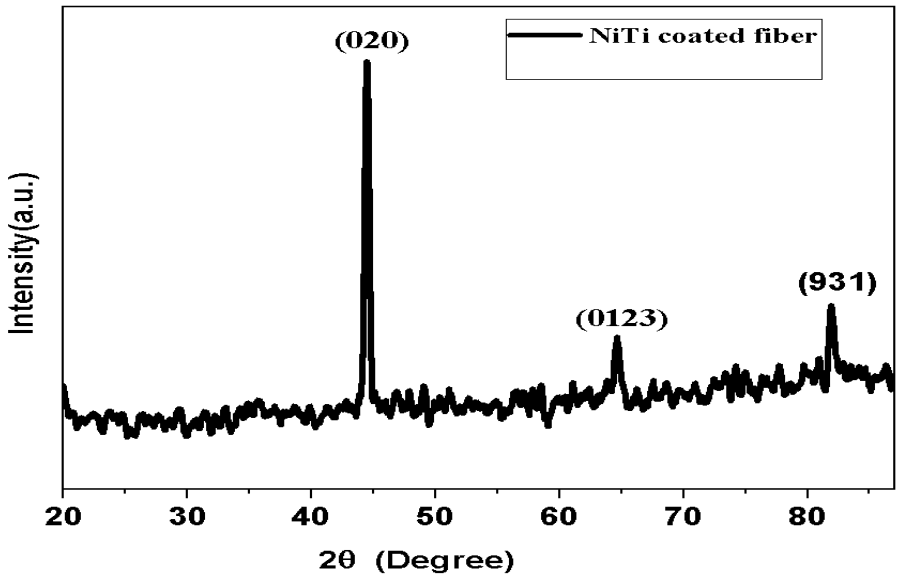

Fig. 13 XRD graph for NiTi coated Fiber

Chapter 5

Mechanical and Shape Memory Alloy Properties of SMA Coated Optical Fiber

5.1 DSC Analysis

5.1.1 For CuAlNi coated fiber

CuAlNi alloy shape memory material undergoes a conversion of austenite to martensite when heated. The lower curve of the DSC plot shows the endotherm during heating cycle (Fig. 14). The austenite peak's start (As) and finish temperature (A_f) are mentioned in the Table 4. These transition temperatures are a function of the alloy composition. There is a hysteresis in the transformation on heating and cooling which is prominent. From the DSC plots (Fig. 14 (a),(b)) it has been observed that there was no martensitic transformation temperature found during cooling cycle of the samples, thus it was due to the effect of polymer and acrylic based optic fiber substrate properties[30]. The coated fiber gradually starts decomposing beyond 250ºC at certain points as due to the cyclic thermal load. The variation of aluminum and nickel composition plays important role in enhancing transformation temperature in the shape memory alloy

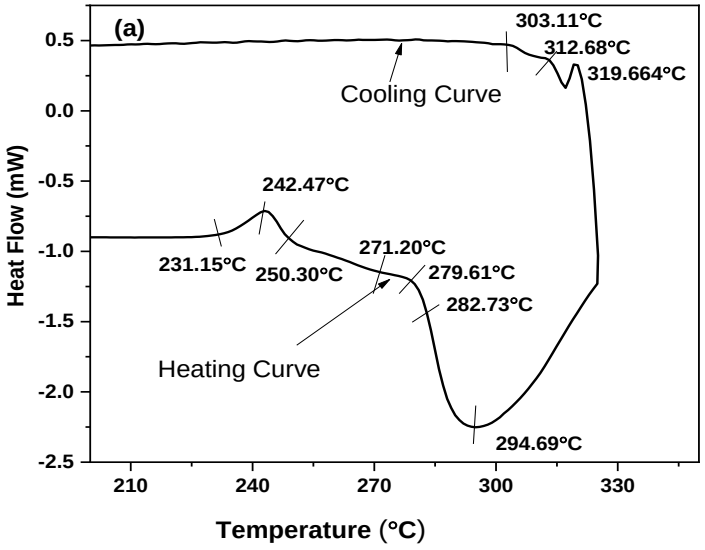

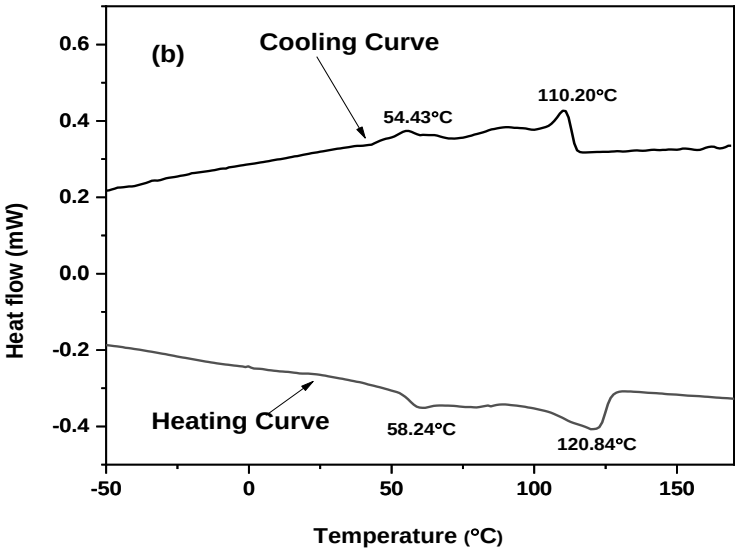

Fig. 14 DSC plot of (a) CuAlNi coated optical fiber and (b) bare optical fiber

property [31,6].

5.1.2 For NiTi coated fiber

Upon cooling, NiTi alloy shape memory material undergoes an austenite to martensite transformation. The lower curve of the DSC plot in the figure below shows the endotherm which results when the sample is cooled at a rate of 10°C per min from 140°C to -50 °C in nitrogen gas flowing at a rate of 25ml/min. On heating, the martensite transforms to austenite which yields an exotherm which can be seen in the upper outline of the DSC plot. These transition temperatures are a function of the alloy composition. Apart from this, another peak is observed at 81°C and at 68.6˚ which may belongs to plastic fiber.

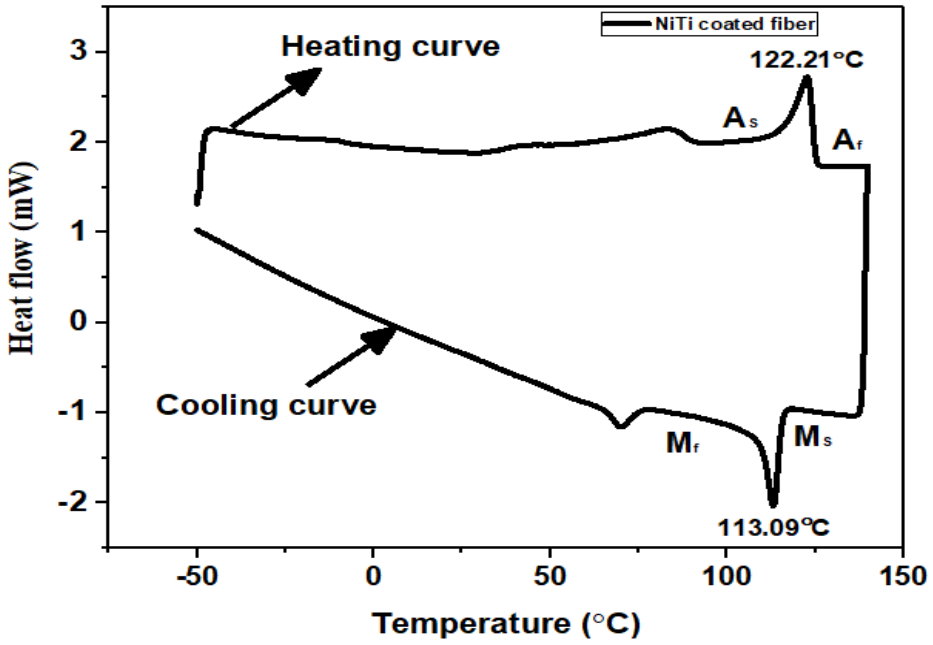

Fig.15 DSC graph for NiTi coated fiber

5.2 TGA result for CuAlNi coated fiber

TGA results for both Cu-Al-Ni coated fibers (at different speeds during deposition) and bare fiber will undergo multiple stage decomposition rate shown in Fig. 16. The rate of decomposition is too less in the initial steps like till temperature 218^0C is almost 5%. After that rapid decomposition occur in case of both bare and the coated fibers. The maximum rate of decomposition takes place in the range of temperature 218^0C to 300^0C in which 40% of weight reduction occurs because of moisture removal or drying process. The curves show increment in mass wherever there is presence of interactive atmosphere like surface oxidation phenomena and a small peak is observed at temperature 440^0C.

Cu-Al-Ni coated fibers has shown greater rate of decomposition and less mass residue than bare coated fiber. It has been observed that due to the alloy deposition, the coated optic fiber exhibits higher degree of heat absorption and results in rapid decomposition when compared to the bare optic fiber. Some nitride compounds formed during this process because

of reaction of polymer's elements (C, H, and O) in the presence of nitrogen [32]. The rapid decomposition of the Cu-Al-Ni sample can be attributed to the ability of the alloys to absorb heat that could lead to the coated samples being conducted. The rapid decomposition of the Cu-Al-Ni sample can be attributed to the ability of the alloys to absorb heat that could lead to the coated samples being conducted.The decomposition temperature profile obtained from the TGA graph has been correlated for equating voltage during electrical actuation. From the TGA results partial melting of CuAlNi coated optical fiber samples has been observed after 190ºC temperature.

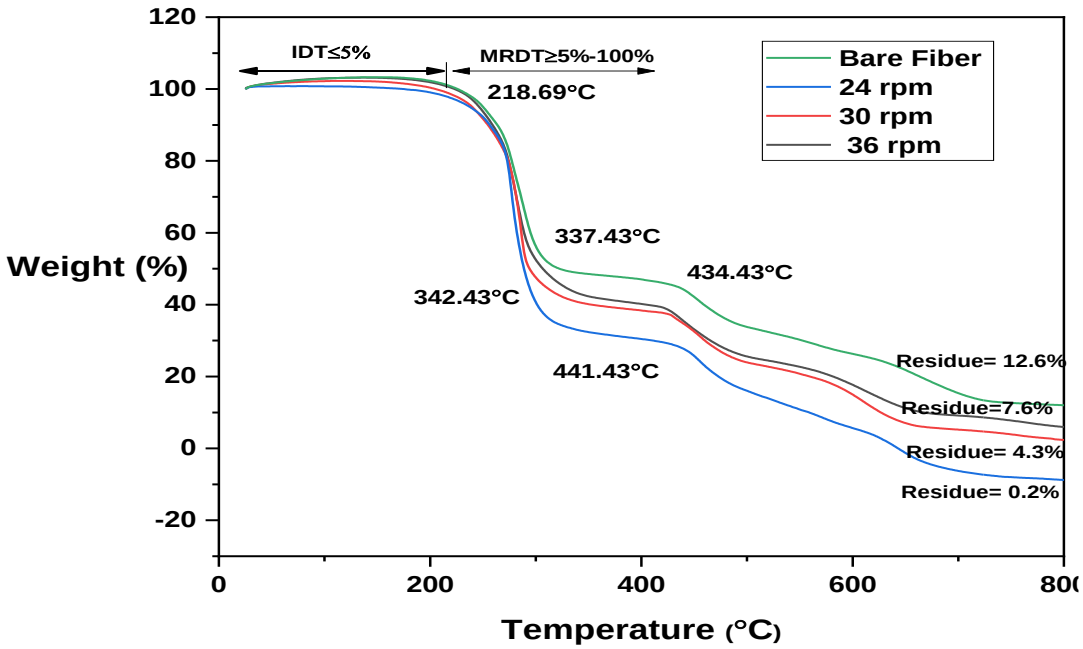

Fig. 16 TGA plot of bare fiber and Cu-Al-Ni coated fibers

5.3 Temperature sensitivity:

5.3.1 For CuAlNi coated fiber

Measurements was made to continuously analyze the behavior of optic fiber in terms of temperature distribution of different samples at different voltage. Fig. 17 shows the thermal images of CuAlNi coated optical fiber during actuation captured with the help of flir one thermal camera and an emissivity of 0.8 has been chosen for coated fiber due to its semi matte

surface [34] .Temperature vs time graph obtained from this non-contact mode of measurement without affecting the film surface gave information about sensing characteristics of different samples which has been coated at varying speed. Electrical actuation comparison has been done based on time requirement for reaching upto highest temperature during heating. In the Fig 18 (a), the sample 3 which is coated at 24 rpm speed showing good actuation in both heating and cooling. Further the fibers are tested under different voltages and the data recorded using DAQ has been plotted on the following graph. From the graph, it has been noted that sample 3 is showing higher actuation temperature at 3 Volt (177ºC) in a very less time. From this observation, it has been concluded that CuAlNi coated fiber sensor samples coated at 24 rpm and actuated at 3V can respond faster with higher thermal conduction than other samples. Other conventional SMA based sensors are not capable to measure this much high temperature in very less time. Thus, the sensitivity of the developed sensor are found to be 0.02mm/ºC and suitable for temperature above 150ºC.

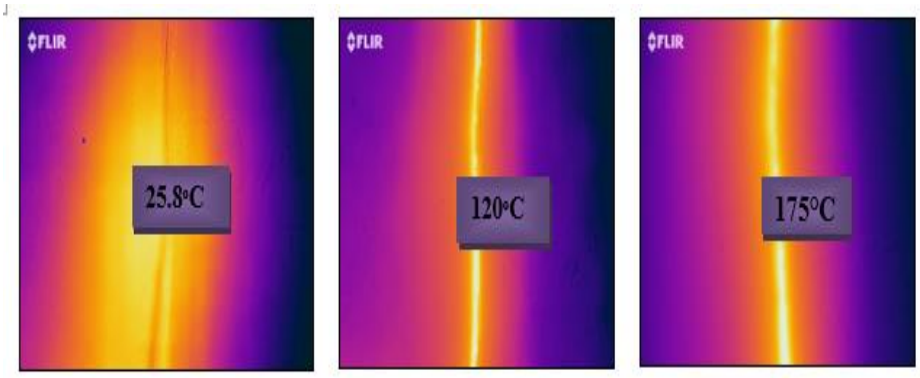

Fig. 17 Thermal images- (a) at starting point heating (b) at mid of the joule heating and (c) at the end of Joule heating

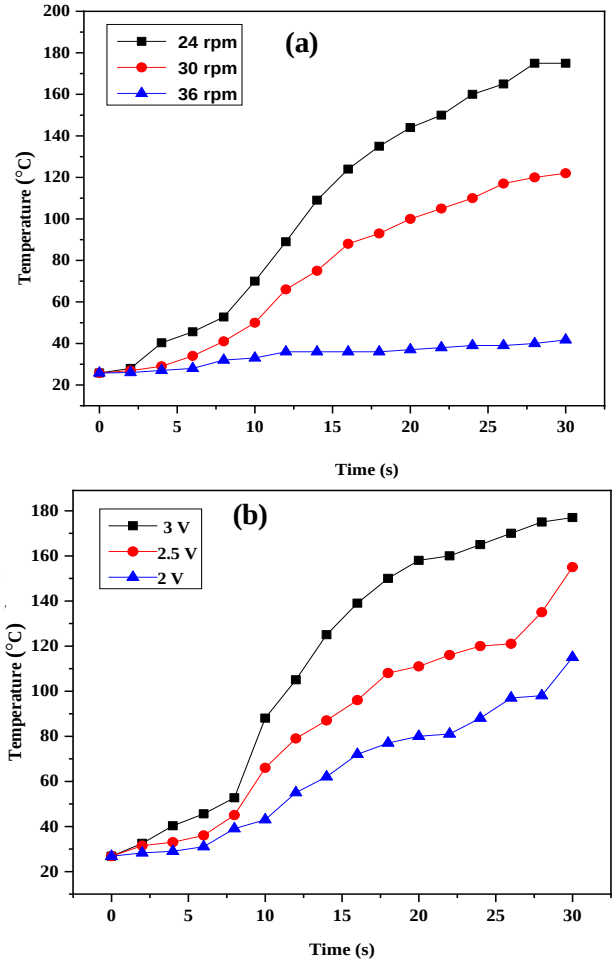

Fig. 18 (a) Time Vs Temperature graph for different samples which has been coated at different speed of in-situ fixture during deposition, (b) Time Vs Temperature graph for coated fiber (24 rpm) at different voltage during Joule heating

5.3.2 For NiTi coated fiber

Thermal images were recorded during this test which is shown in Fig.19 with the help of flir one thermal camera. For this semi-matte surface selected surface emissivity was 0.8 [10].Calculated sensitivity for NiTi coated optical fiber was 0.016 mm/˚C [11]. From this observation it has been proved that SMA coated fiber based sensor can work in higher temperature.

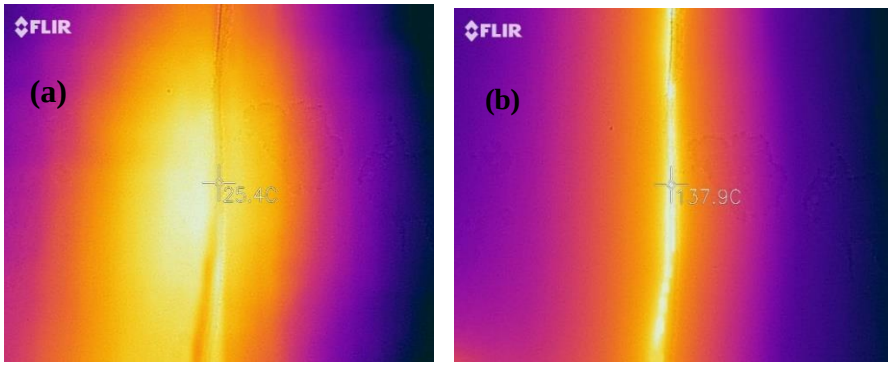

Fig. 19 Thermal Imaging of NiTi coated Optic Fiber (a) at the start of heating, and (b) at the end heating

5.4 Stress and Strain curve

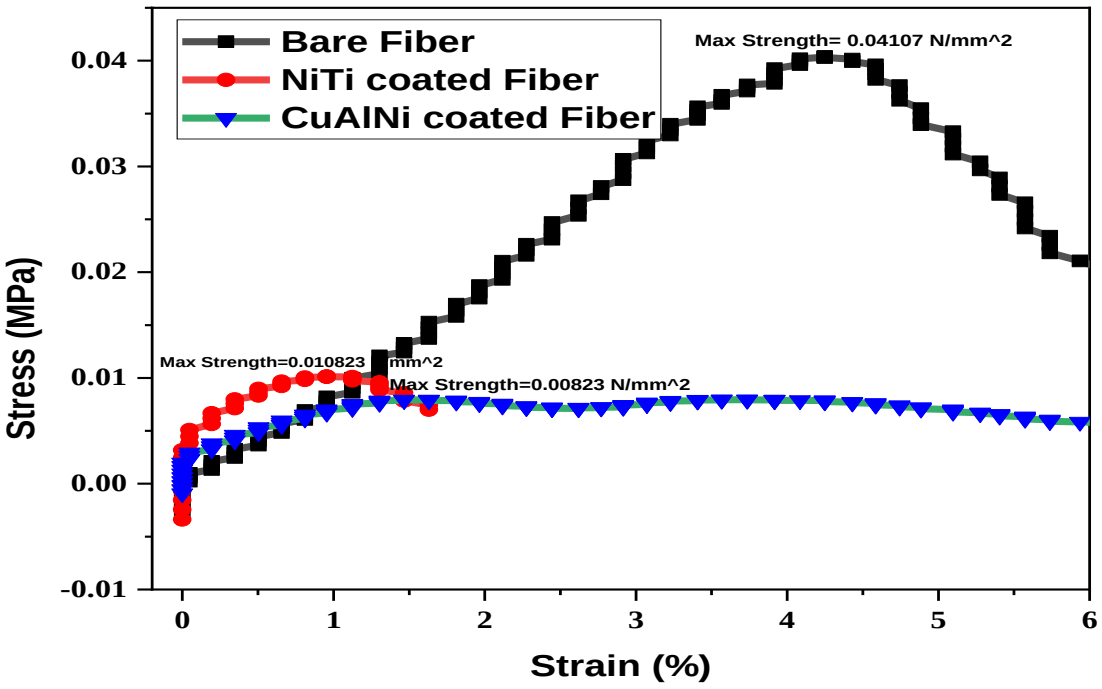

Fig. 20. Stress and Strain curve of bare fiber ,CuAlNi and NiTi coated fiber

Tensile test is carried out to observe the mechanical properties of the three forms of fibers: bare fiber, one with a coating of CuAlNi SMA and the other with a covering of SMA NiTi. The stress vs strain curve is plotted as in Fig. 20. The shape memory alloys having base as copper, such as

CuAlNi, have comparatively poor mechanical properties than those of NiTi which, in turn, have poor mechanical properties as compared to that of bare fiber. The ultimate tensile strength of the bare fiber can be observed going up to 0.04107 N/mm^2, while those of NiTi and CuAlNi coated fiber are constrained to 0.010823 N/mm^2 and 0.000823 N/mm^2. Due to the small elastic anisotropy and small grain size, NiTi coated fiber has a high ductility as compared to that of CuAlNi. The CuAlNi coated fiber, on the other hand, is brittle because of the large anisotropy and large grain size. As can be seen from the curve, the area under the curve of bare fiber is the maximum, indicating that it has maximum fracture toughness, i.e., it can absorb the maximum amount of energy before fracture. As the thin film stretches over a certain limit, the SMA film peeled off from fiber in tensile testing. Deformation induced martensite to martensite and reorientation of martensite represents the linear rise in stress with strain. The deformation of martensite phase is responsible for the deformation of the composite thin film and then after reaching the elastic limit, the fracture occurs. The bare fiber being tougher (and thus stiffer) than the CuAlNi or NiTi coated fiber, is the least flexible.

Chapter 6

Thermomechanical Behavior of Shape Memory Alloy Coated Fiber Under Hot Plate and Electrical Actuation

6.1 Hot Plate Actuation:

6.1.1 For CuAlNi coated fiber

For evaluating the thermal actuation hot plate analysis has been used. During the deposition process optical fiber has been fixed with motor drive fixture, which was in twinned martensite state, the schematic of shape memory effect on coated optical fiber shown in Fig. 2. After coating, the optical fiber has been removed from the fixture, which resulted in detwinned martensite (semi-curved shape) due to thermal stress of SMA deposition. The coated optical fiber was kept on hot plate at 190^{o}C temperature. The coated fiber become straight due to heating but after removal from hot plate, it has regained its original shape (semi-curved shape). On hot plate actuation, sample prepared at the lowest fixture drive velocity has achieved more actuation in 6 seconds. This temperature is lower than DSC transformation temperature this is due to differences to residual stresses induced in CuAlNi thin film by optical fiber during fabrication process. In the Fig. 21 ,there is a change in bending angle with respect to temperature has calculated with the help of hot plate. During this experiment one end of the coated fiber was fixed and there is change in bending angle at one end due to shape memory effect during heating and cooling. A maximum change in bending angle of 59.1^{o} was achieved for SMA coated at 24 rpm and minimum shape recovery ratio observed was 16.27 ^{o} for the sample which had highest speed (36 rpm) during deposition. The fiber which has been coated at lowest speed during deposition showing better actuation result in both heating and cooling was further tested for electrical actuation. The CuAlNi have

higher conductivity because of which it can absorb more heat during heating which will give higher actuation. In NiTi based alloys the heat transfer rate is less which echoes in their shape recovery. Transformation temperature has decided the change in bending angle of SMA coated fiber. Also from the hot plate actuation, after 200ºC the coated optic fiber starts melting and the same has been observed from the Thermo Gravimetric Analysis (TGA) results.

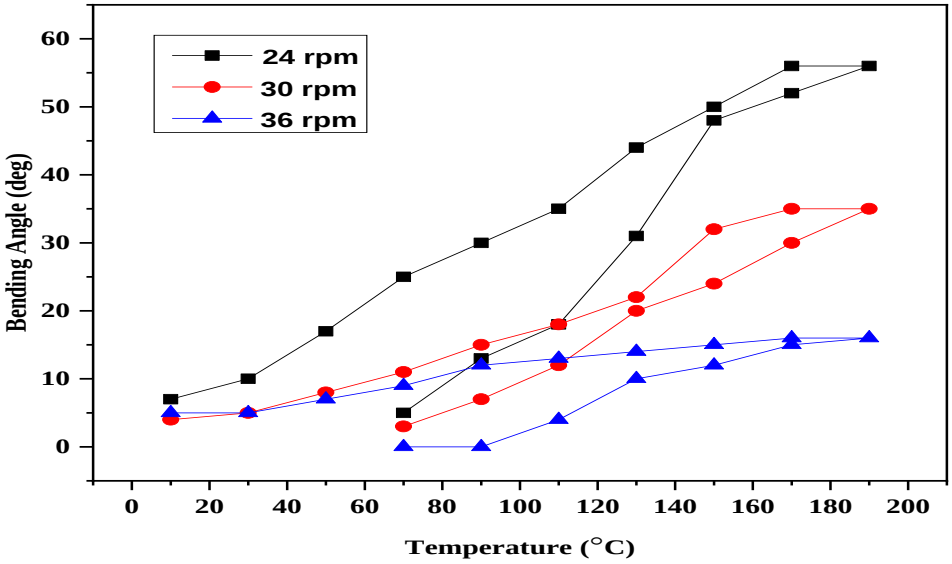

Fig. 21 Change in bending angle vs Temperature graph

6.1.2 For NiTi coated fiber

Hot plate analysis has been conducted for evaluation of thermal actuation. During the deposition process the optical fiber was fixed with in-situ fixture during deposition it was in twinned martensite state. After deposition, coated fiber was in detwinned martensite because of thermal stress which generated during deposition. Both SMA coated fiber was heated upto 150˚C.On heating the fiber will become straight and after removal from hot plate it will regain its original shape. This temperature is different from the DSC phase transformation temperature because of induced stress during fabrication process. During this test one end of fiber is fixed and displacement for other end was recorded. In the Fig. 22, the graph in between change in displacement with respect to temperature NiTi

coated has plotted with the help of hot plate. In NiTi based alloys the heat transfer rate is less which echoes in their change in bending angle. Transformation temperature has decided the shape recovery ratio of SMA coated fiber.

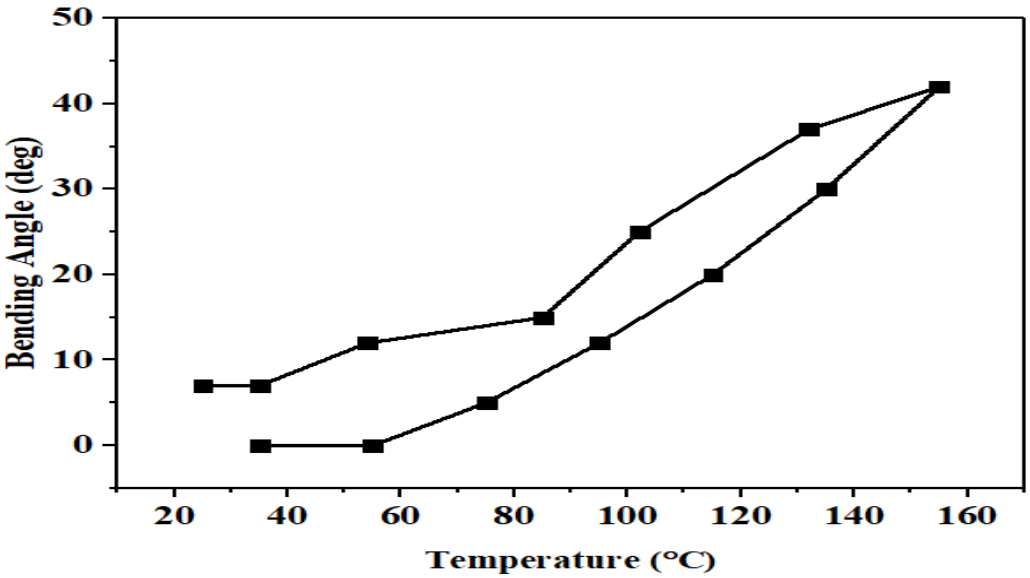

Fig. 22 Change in bending angle vs temperature graph

6.2 Electrical Actuation test:

In this work, Joule heating or resistive heating technique has been used to actuate the coated optical fiber. The coated fiber was wounded with lightweight aluminum wire of diameter 0.05 mm. For the electrical actuation-based displacement measurement, one end of the fiber has been fixed to the clamp and the other end has been kept movable with feasibility of adding varying load in a cantilever fashion. Whereas a difference in potential has been applied to both the ends of the aluminum wire and then electrical actuation was carried out by varying voltage and load. Due to this effect the applied electrical energy over the aluminum wire contact is converted into thermal energy over the fiber surface. In addition, based on the applied electrical input, subsequent displacement was obtained in the optic fiber through shape memory effect. Thus based

on the variation in actuation parameter inputs, altering load and their respective displacement output the developed fiber has been tested for real-time dynamic measurements [33,34]. The heating effect has been mentioned as in the following equation.

$$\boldsymbol{H = i^2RT}$$

Where,

H – Heat energy

i – Current flow in the circuit

R – Resistance of the circuit

T – Time of current flow in the circuit

6.2.1 For CuAlNi coated fiber

The copper-based alloy requires less power for actuation in comparison to NiTi because of its lower resistivity and light weight. Above 3.5 V, the high temperature produced has led to the removal of CuAlNi coating from the fiber surface. Therefore, the voltage between 2 to 3 V was selected for actuation. The thermomechanical behavior of the Cu-Al-Ni coated optical fiber was tested under various actuation conditions with varying loads of 25 mg, 50 mg and 75 mg at different voltages of 2V, 2.5 V and 3 V to evaluate the maximum displacement as shown in Fig. 23(a),(b) and (c). It was inferred from the response that Cu-Al-Ni coated fiber requires a maximum actuation of 3.2 s and a minimum of 0.4 s, indicating the time needed to reach the austenitic phase. The cooling curves indicate that, under most actuation circumstances, the optical fiber returns to its original position with a marginal displacement loss. The optimized parameter for peak displacement is 3 V, 2.5 A at a load condition of 25 mg from this thermomechanical consequence. Samples from Cu-Al-Ni show a constant actuation. The heat energy generated in the optical fiber is proportional to the current square, which means that a small increase in current dramatically increases the coated fiber's internal temperature, resulting in an enhanced recovery of the shape. When compared to hot plate actuation,

the electrical actuation shows reduced displacement due to the non-uniform heat profile across the fiber as the temperature applied over the fiber in the form of coil gets varied across the circumference. CuAlNi coated optical fiber having higher displacement in comparison to NiTi coated optical fiber because of lower resistivity. CuAlNi was shown better actuation characteristics because of their larger grains in comparison to NiTi which will help in martensite transformation.

Table 7 Voltage vs maximum displacement characteristics for different loads for CuAlNi coated Fiber

Load	Voltage (Volt)	Maximum Displacement (mm)
25 mg	2	2.02
	2.5	2.97
	3	3.7
50 mg	2	1.9
	2.5	2.46
	3	2.9
75 mg	2	1.79
	2.5	1.89
	3	2.25

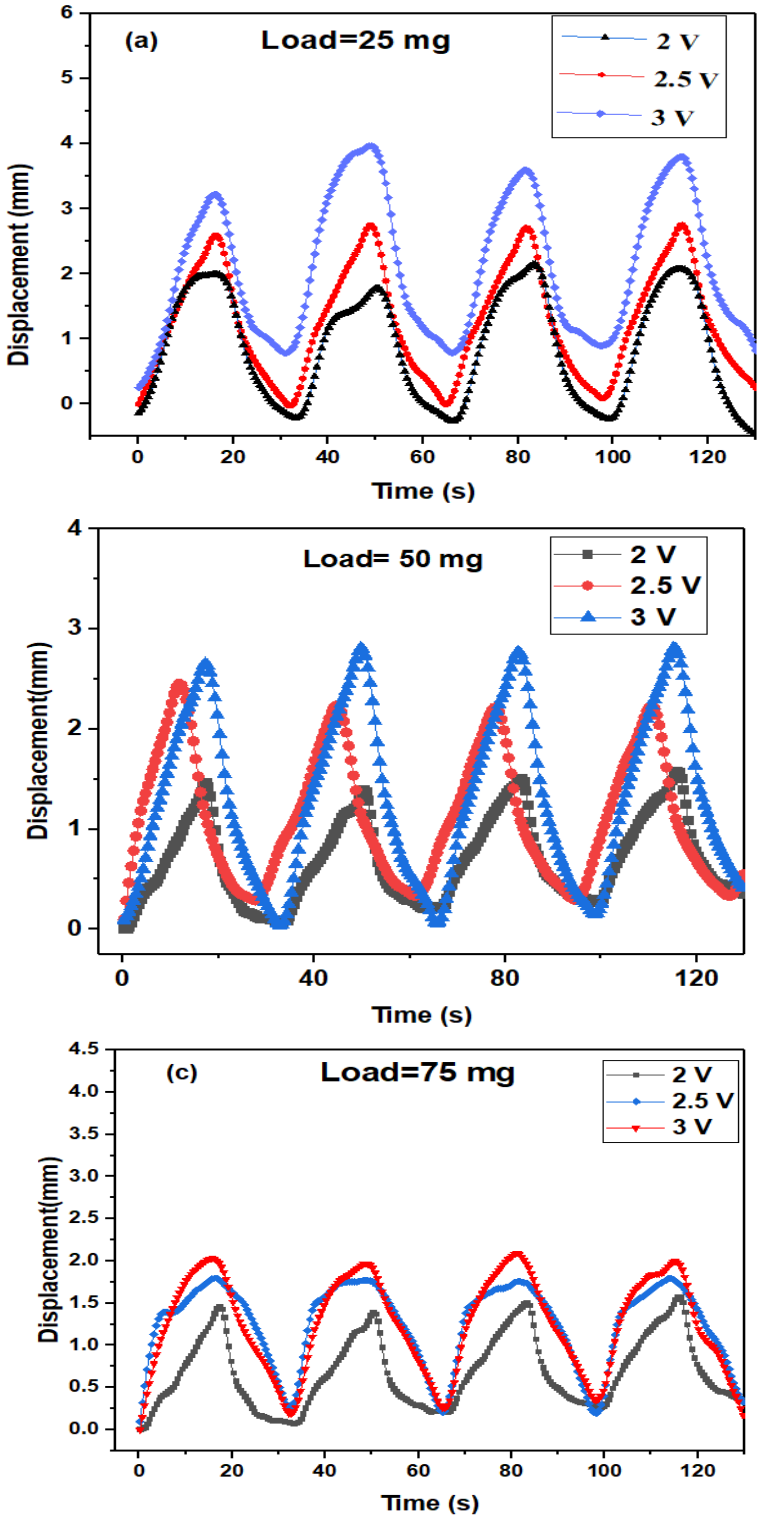

Fig. 23 Actuation behavior of coated optic fiber with (a) 25mg, (b) 50mg and (c) 75mg at varying voltage

6.2.2 For NiTi coated fiber

The Thermo mechanical test was conducted for NiTi coatd fiber under various conditions with varying loads of 35 mg, 50 mg and 75 mg at different voltages 2 V,2.5 V and 3 V.

NiTi coated optical fiber acts instantly, showing a greater sensitivity to Jou le heating with quicker kinetics of conversion as shown in Fig.24.With the increment of load displacement reduced because that load was resisting the moment during the experiment. The NiTi coated optical shows stable actuation with respect to load increment. Fig. 8 shows the actuation result upto 15000 cycles which is showing reliability and fatigue life results of NiTi coated fiber which is showing upto which cycle the fiber can actuate.The life cycles of NiTi were analysed using electrical actuation. The NiTi coated fiber required upto 15000 cycles to reach a displacement of 95% of the initial value after which coating got peeled off or it fractured as shown in Fig. 26. Life cycle test was performed for one sample at two different voltages.

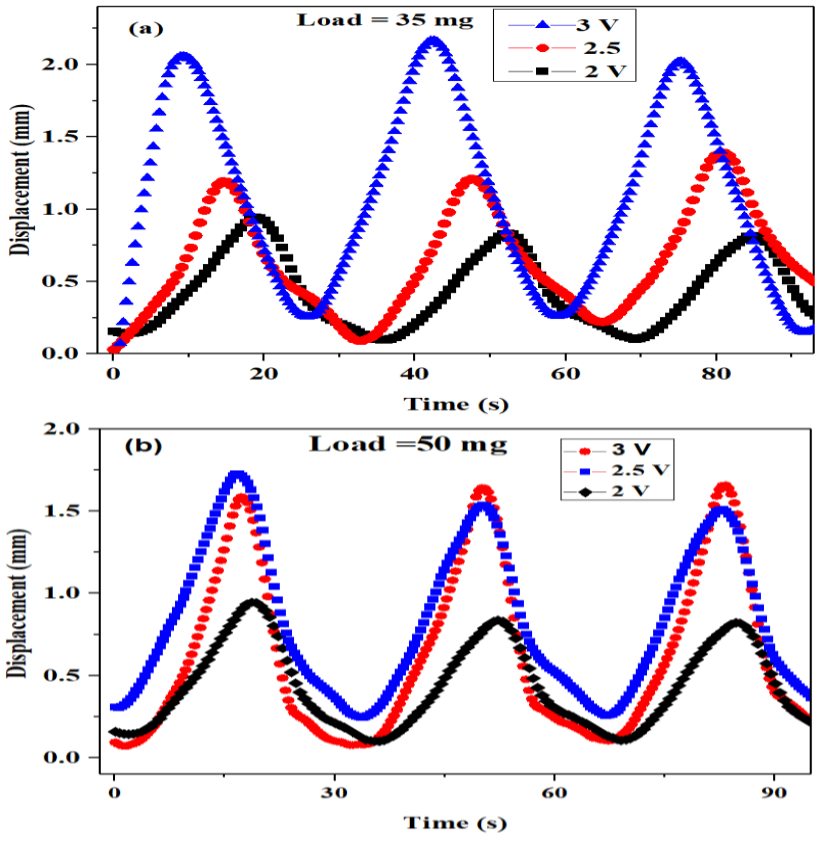

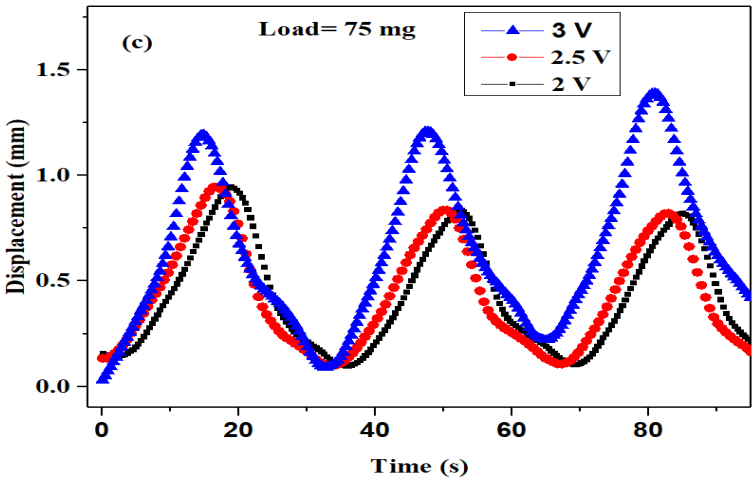

Fig. 24 Actuation behavior of coated optic fiber with (a) 35 mg, (b) 50mg and (c) 75mg at varying voltage for NiTi coated fiber

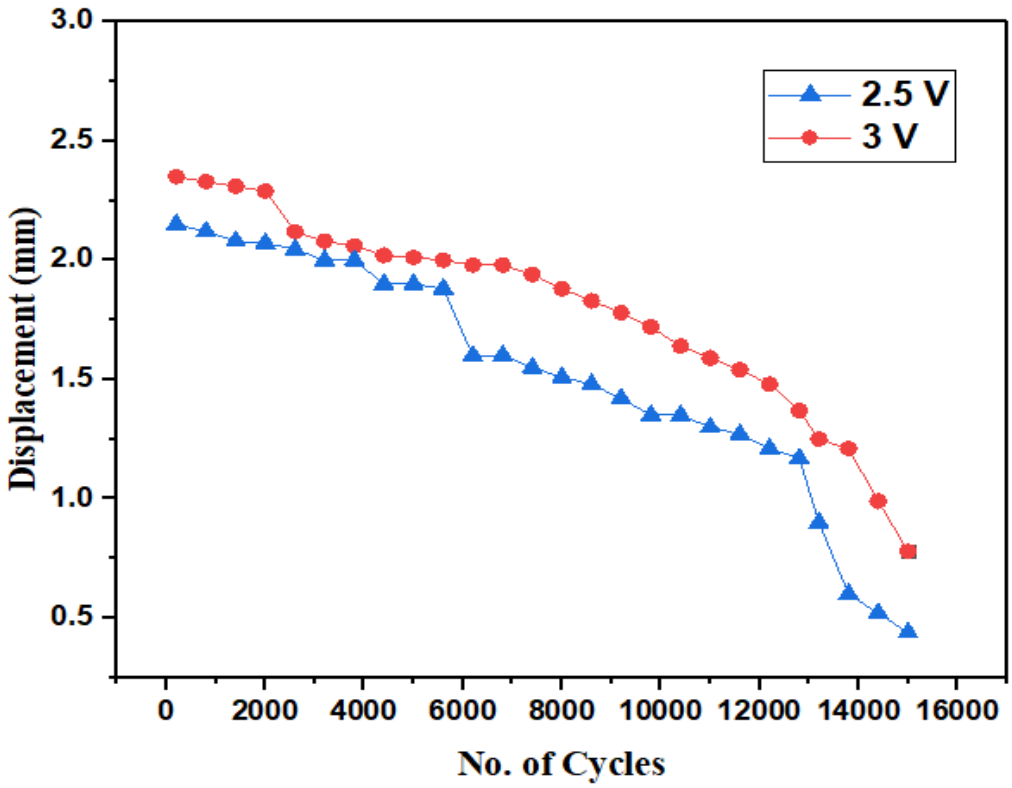

Fig. 25 Life cycle behavior of NiTi coated fiber upto 15000 cycles

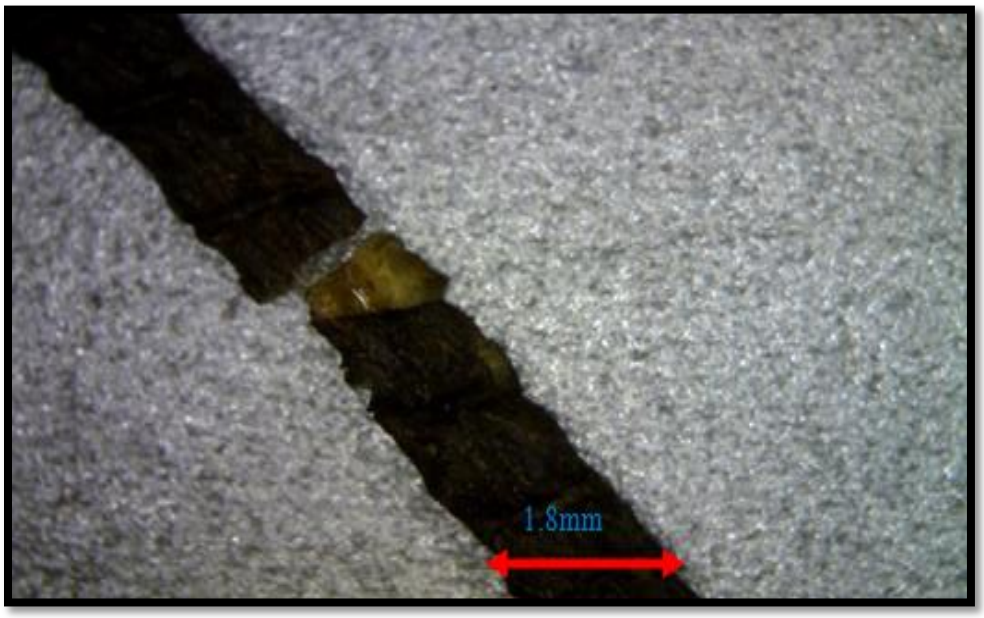

Fig. 26 Sample after Life cycle behavior

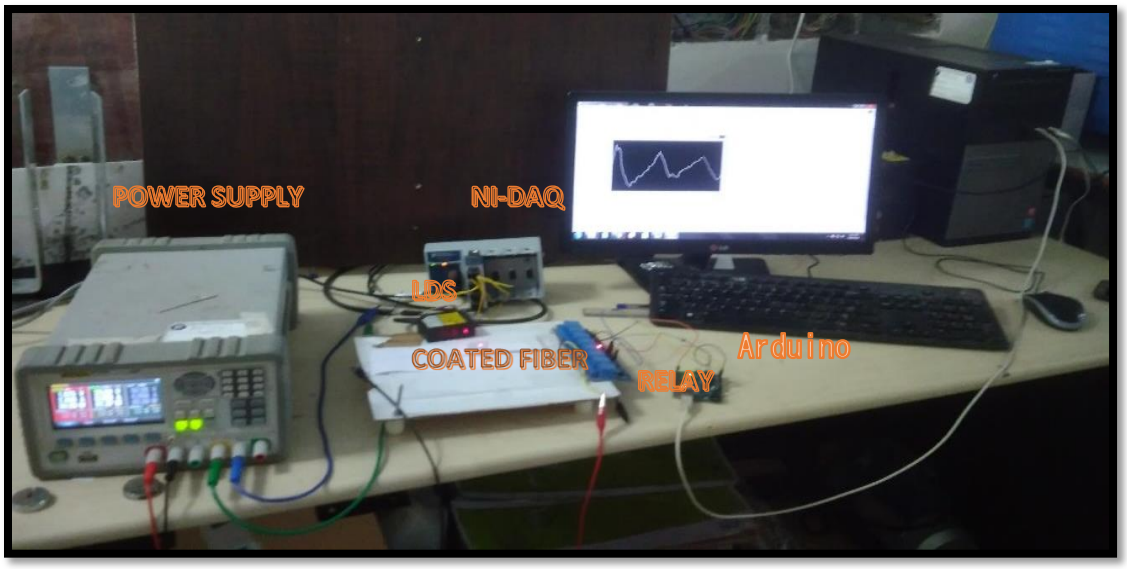

Fig. 27 Real time diagram of life cycle analysis

Table 8: Voltage vs Maximum Displacement characteristics on load variation for NiTi coated Fiber

Load (mg)	Voltage (Volt)	Maximum Displacement (mm)
35	3	2.25
	2.5	1.45
	2	1
50	3	1.80
	2.5	1.2
	2	0.9
75	3	1.35
	2.5	1
	2	0.80

Chapter 7

Sensing result of Shape Memory Alloy Coated Fiber

In this work an experimental test bench was developed to use for validating the developed SMA coated optic fiber samples.Non -contact mode of sensing approach was used to study the SMA coated fiber optic samples. Heating coil made up of Nichrome wire of 15 cm length and 0.50 cm coil diameter with 50 turns and was used to generate heat around the optic fiber. The fiber was coupled at both the ends using 3D printed coupling parts with the collimator and the pin hole detector. A 650 nm wavelength based red led light emitting diode was used to generate light at the source side. Also a photo transistor PT 333-3C everlight make was used to measure the light intensity in terms of equivalent current at the output side. The results were observed for displacement vs intensity to study the thermo-optic coupling response of the developed smart optic fiber sensor. This method of SMA deposition over optic fibers proves higher spectral shift due to improved thermal sensitivity of the fabricated sensor than pure metal coated or other alloy coatings [26]. From the resulting graph mentioned in Figure 17. it has been observed that for increasing displacement in the SMA coated optic fiber sensor, the light intensity varies and thus it affects photon energy with subsequent reduction in output current [45]. Further to study the losses occurred due to airgap during optic fiber coupling at both the ends also has been proposed to collimate appropriately.

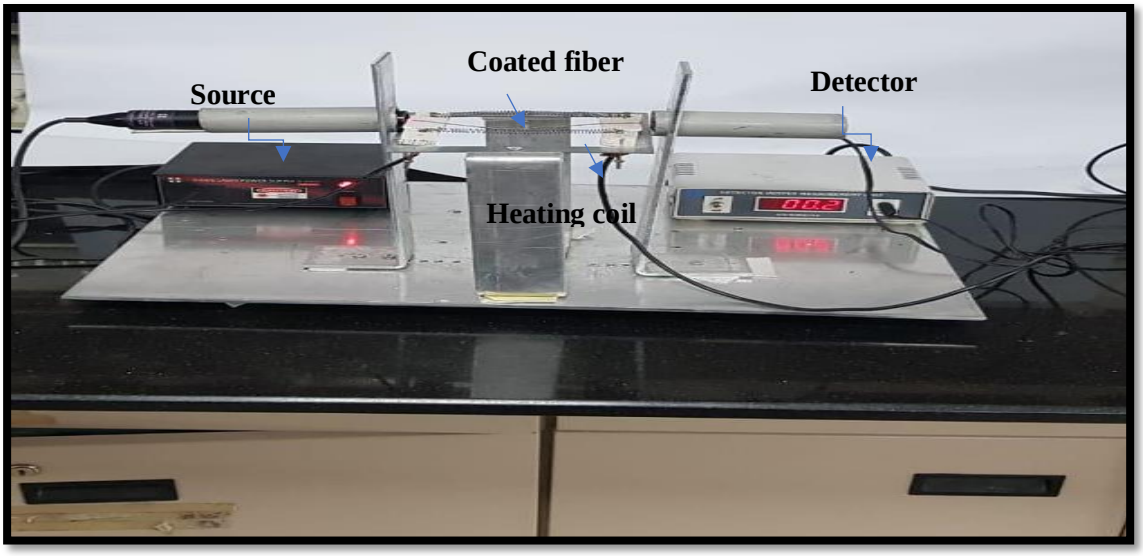

Fig. 28 SMA Coated Optic Fiber Sensing Setup

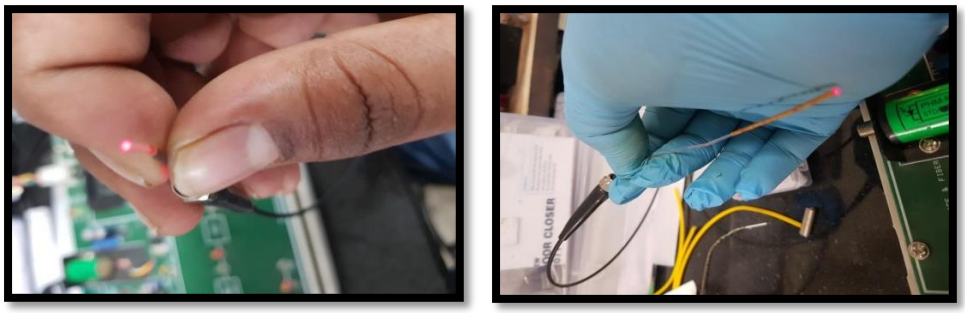

Fig. 29 Light Transmission via Coated Optic Fiber

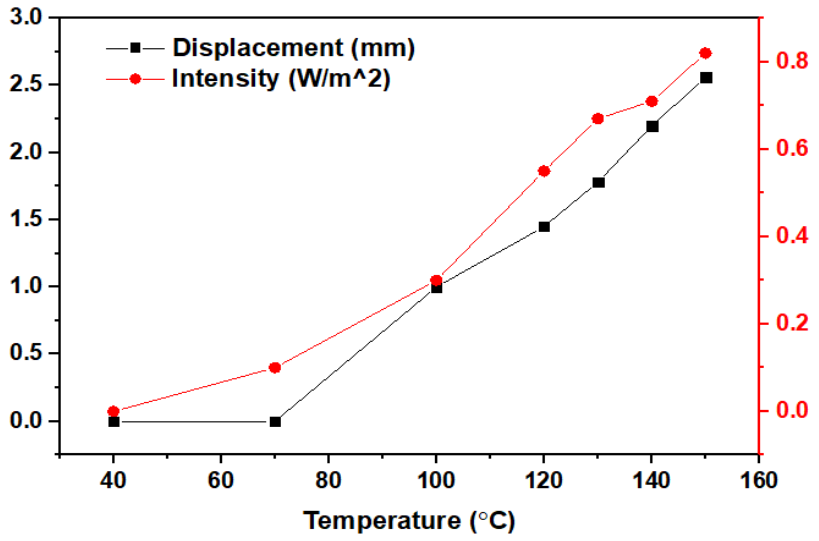

Fig. 30 Displacement vs Output Intensity Graph on Temperature scale for the NiTi coated

Optic Fiber

Commercially sensors are characterized using its properties and special attributes such as sensitivity, precision, accuracy etc. In this work the developed Cu based SMA coated optic fiber sensor was studied for precision using life cycle analysis upto 5000 cycles. Electrical actuation was performed to study the cyclic behavior and fatigue life of the SMA coated optic fiber. The developed sample was tested at 2.5Amp, 3volt and at a load of 75mg. Maximum and minimum displacement of 4.92mm and 1.7mm was observed from the resulting graph (Fig. 31). From the life cycle analysis, it can be observed that the optic fiber has stable actuation behavior with fluctuation and the displacement was constantly varying during actuation at varying frequencies and voltage. Even after 5000 cycles there was no saturation in the response. From the displacement presented a steady and stable actuation behavior throughout the 5000 cycles was realized. These results obtained from the experimental evaluation proves that the high precision temperature measurement using shape memory alloy coated optic fiber sensor are feasible

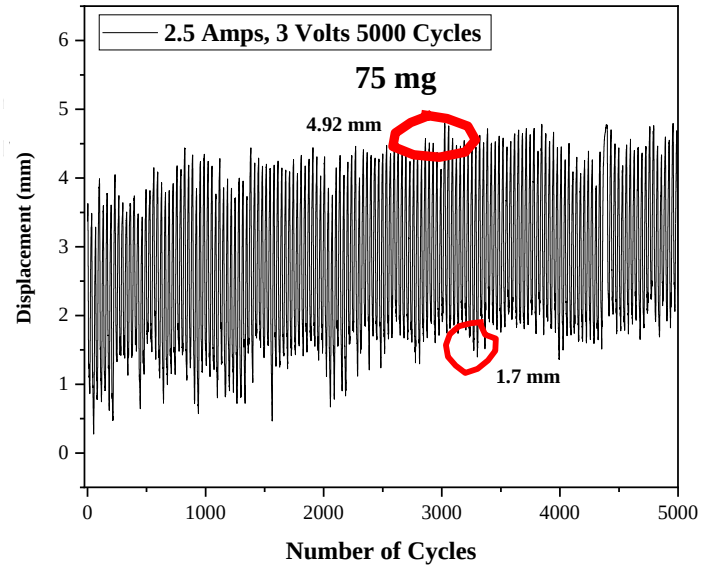

Fig. 31 Life cycles analysis of the CuAlNi SMA coated Optic Fiber Sensor

Precision of the developed CuAlNi coated optic fiber sensor was tested using in house developed fiber optic sensing test bench. The test bench consists of light source and photodetector coupled with SMA coated optic fiber and also adjacently actuated using heater coil made up of nichrome wire. The heater coil has been placed at a distance of 2.5cm from the optic fiber such that the fiber can sense the temperature in the non-contact mode. The photodetector voltage and current readings were continuously assessed and monitored using data acquisition system (Make: NI CDAQ 9219). Using arduino uno program has been made to operate the heater coil at a 50% duty cycle for 3.84 sec on and 3.84 sec off timing to actuate the SMA coated optic fiber for heating and cooling mode.

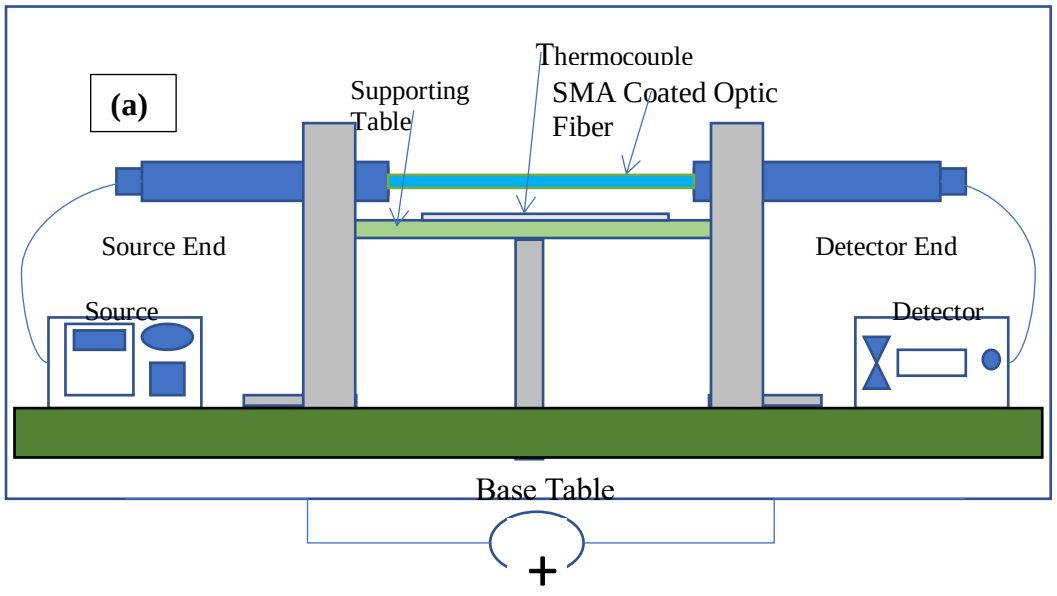

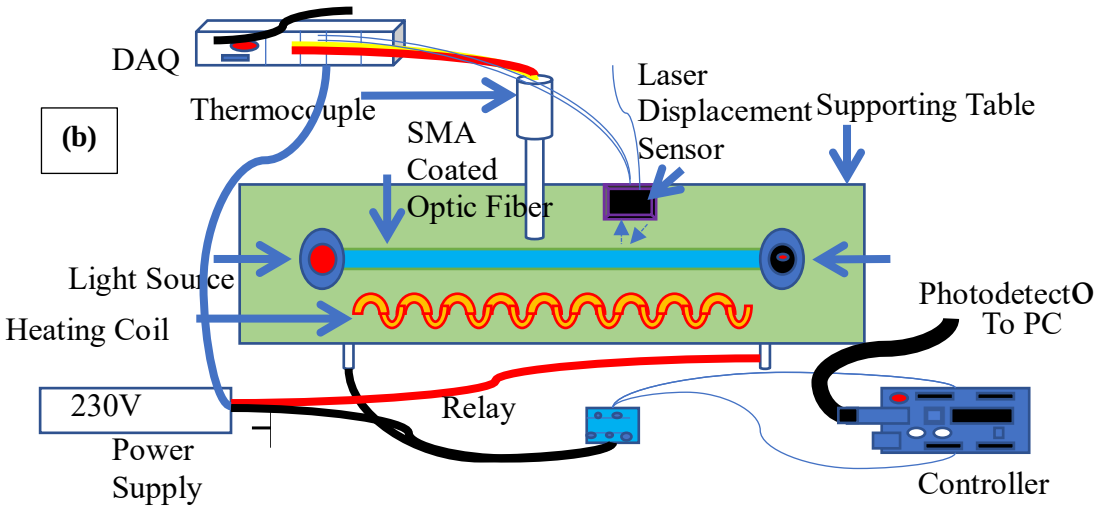

Fig. 32 Test bench for temperature measurement of the optic fiber sensor (a) Side View (b) Top View

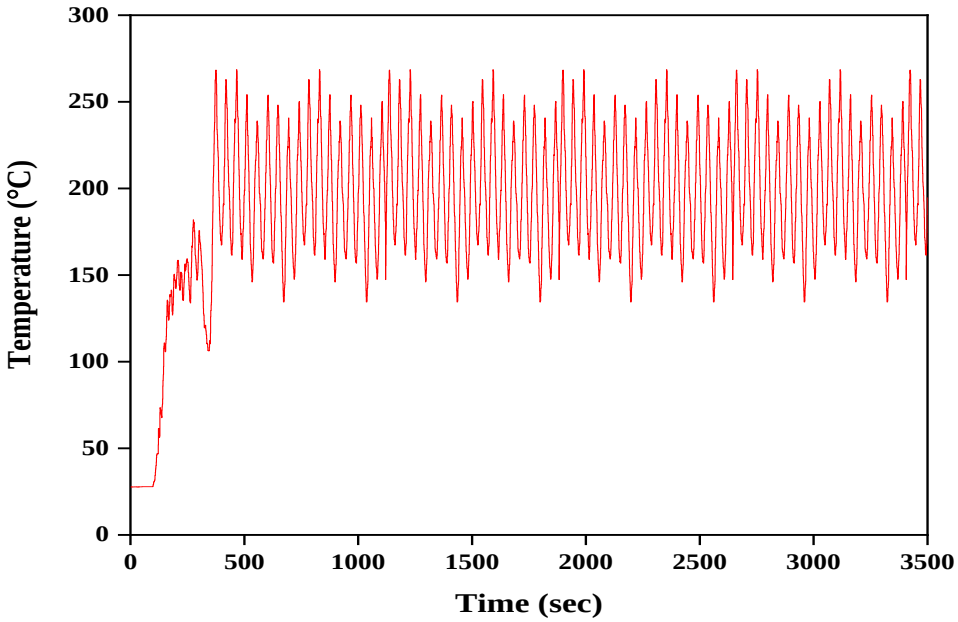

Fig. 33 Temperature Cycles during SMA Sensing

The temperature cycle used for optic fiber sensing setup has been measured continuously using thermocouple of K-type. For more than 100 cycles the temperature readings with respect to heating and cooling cycles experiment have been performed to measure the fiber sensor readings. From the graph it has been observed that for the first 100 sec there was a delay in rise time as the sensor gets measured from room temperature.

Then continues cycles are measured in the range of 140°C to 280 °C where the transformation from the thermal analysis also found suitable.

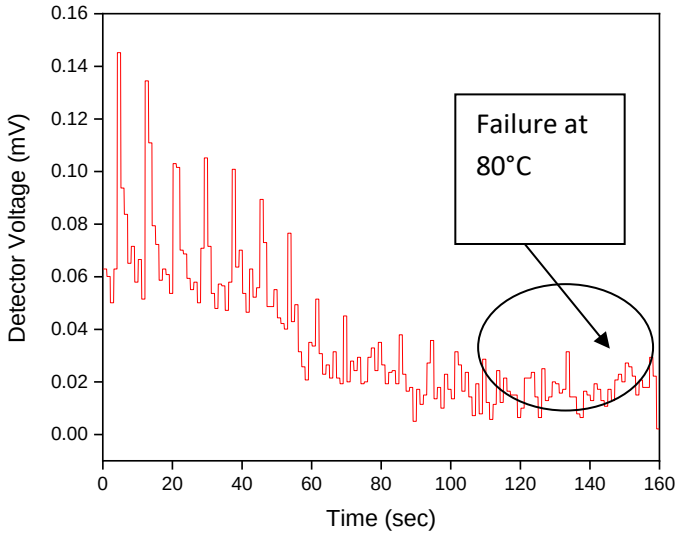

Fig. 34 Signal Response of the Bare Optic Fiber

Using the same thermo-optic test bench bare optic fiber also tested for temperature measurement. But in this case of bare optic fiber the signal gets deteriorated and gets unavailable at 80°C as the fiber got failure.

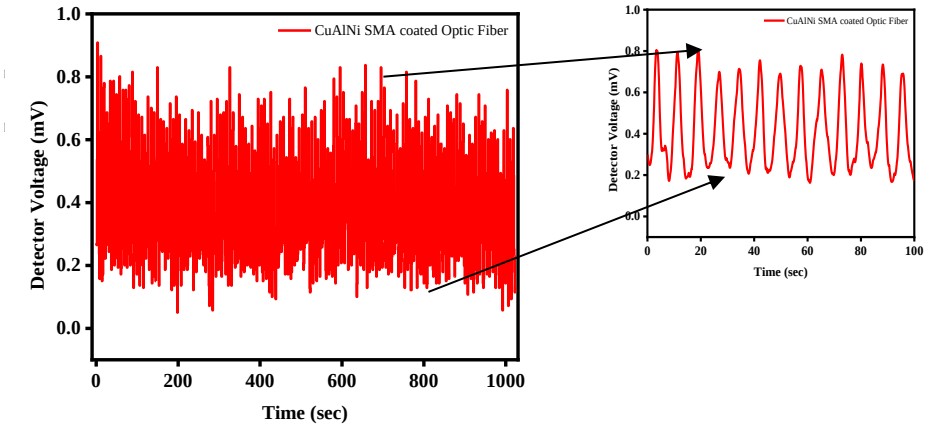

Fig. 35 Precision analysis of the CuAlNi SMA coated Optic Fiber Sensor

The developed samples have been tested for more than 125 cycles in which the output of the fiber has been found precise for the entire cycles. During normal room temperature the output of the SMA coated fiber was 0.2mV while during actuation the fiber produces 0.8mV at the austenite phase condition. Thus the developed sensor was more precise than that of the other standard thermal sensor with its noise rejection and quick response capabilities

Chapter 8
Conclusion and Future scope

8.1 For CuAlNi coated fiber integrated sensor

From the above experimental results, it can be accomplished that Cu-Al-Ni coated optical fiber developed through flash evaporation showed cyclic periodicity.

The results are encapsulated as

- The surface morphology of the coated optical fiber is continuous, smooth and has layered surface with a grain size of approximately 150 nm.
- High intensity peaks corresponding to (128) and the crystallite siz e was found to be 5.14 nm from the XRD graph showing the crysta llinity of the structures developed.
- The thermal decomposition of the Cu-Al-Ni/Plastic optic fiber was higher compared to bare optic fiber as confirmed by TGA analysis.
- Upon calculation of the change in bending angle, it was found that varying speed of 24 rpm has better recoverability than that of 30 rpm or more.
- Using an electrical actuation setup, the optic fiber composite was examined for varying voltages and currents at different loads, the cyclic behavior was studied. Moreover, the fiber showed slight signs of deviation from the average displacement.
- The electrical actuation of SMA optical fiber has shown a maximum displacement of 3.7 mm.

8.2 For NiTi coated fiber Integrated sensor

From the above experimental results, it can be accomplished that NiTi coated optical fiber developed through flash evaporation showed cyclic periodicity.

The results are encapsulated as

- From the SEM results the surface morphology of the coated optical fiber is continuous, smooth and has layered surface with a grain size of approximately 330 nm.
- The fiber coated with NiTi exhibits monoclinic structure in martensite phase, rhombohedral structure in R phase and cubic structure in austenite phase. Due to the presence of R phase, the two-way shape memory effect is enhanced in NiTi.
- From the DSC examination, the austenite change temperature for NiTi was observed to be 122.3˚C and martensite begin temperature was 113.0℃.
- An electrical actuation was used to study the cyclic behavior. It too k less time for NiTi to start operating and showed a peak displacem ent of 2.25 mm.
- Calculated sensitivity for NiTi coated fiber-based sensor is 0.025 mm/˚C.

8.3 Future scope

The fabricated smart fibers are suitable for use in sensing applications in various high temperature process control applications. As a proposed work, Fig. [31] shows a continuous system for the application of pipeline temperature monitoring has been considered with a working range of around 200ºC in order to monitor the transfer temperatures and for leakage assessments. The smart fiber optic sensor will be layered underneath the pipeline structure so that leakages at any of the circumference of the pipe will bring it down due to gravity and it can sense the variant in parameter easily. The pipeline surface temperature will cause micro bends and deflection in the smart sensor which will further induce changes in the

wavelength of the optic signal and it can be measured using the shift in the spectrum changes.

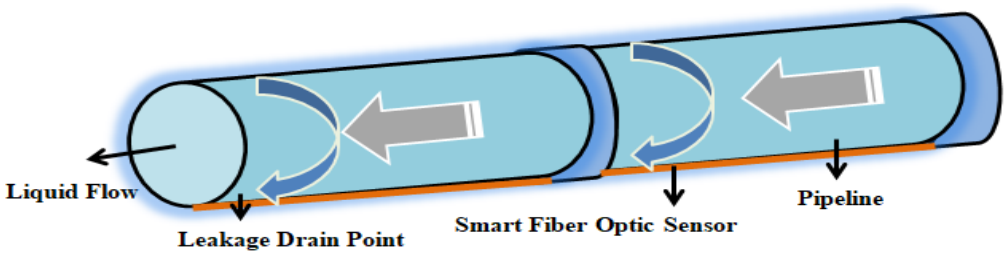

Fig. 36 Fiber optic sensor for pipeline temperature sensing

Chapter 9

References

1. K.S.C. Kuang, W.J. Cantwell, The use of plastic optical fibers and shape memory alloys for damage assessment and damping control in composite materials, Meas. Sci. Technol. ,2003 ,14, 1305–1313. doi:10.1088/0957-0233/14/8/316.
2. K.S.C. Kuang, S.T. Quek, W.J. Cantwell, Active control of a smart composite with shape memory alloy sheet using a plastic optical fiber sensor, Sensors Actuators, A Phys. 2013 ,201 , 182–187. doi:10.1016/j.sna.2013.06.024.
3. D. Inaudi, B. Glisic, Long-Range Pipeline Monitoring by Distributed Fiber Optic Sensing, J. Press. Vessel Technol. 2010, 132 , 011701. doi:10.1115/1.3062942.
4. F. Scurti, J. McGarrahan, J. Schwartz, R. Wang, A.R. Caruso, M. Breschi, G.M. Zhang, U.P. Trociewitz, H.W. Weijers, J. Schwartz, 12 S Mahar, J. Geng, J. Schultz, J. Minervini, S. Jiang, P. Titus, M. Takayasu, C.-Y. Gung, W. Tian, A. Chavez-Pirson, Effects of metallic coatings on the thermal sensitivity of optical fiber sensors at cryogenic temperatures " Real-time simultaneous temperature and strain measurements at cryogenic temperatures in an, Opt. Mater. Express. 2017, 9 , 57–79. doi:10.1364/OME.7.001754.
5. P. Way, Effects of metallic coatings on the thermal sensitivity of optical fiber sensors at cryogenic temperatures, M. Science, 2017, 7, 1754–1766.
6. S.N. Saud, E. Hamzah, T. Abubakar, H.R. Bakhsheshi-Rad, S. Farahany, A. Abdolahi, M.M. Taheri, Influence of Silver nanoparticles addition on the phase transformation, mechanical properties and corrosion behaviour of Cu-Al-Ni shape memory alloys, J. Alloys Compd. 2014 ,612 , 471–478 , doi:10.1016/j.jallcom.2014.05.173.
7. A. Ishida, Ti-Ni-Cu/polyimide composite-film actuator and simulation tool, Sensors Actuators, A Phys.,2015, 222, 228–236, doi:10.1016/j.sna.2014.12.012.
8. Ishida, M. Sato, Ti-Ni-Cu shape-memory alloy thin film formed on polyimide substrate, Thin Solid Films. , 2008 , 516 , 7836–7839,

doi:10.1016/j.tsf.2008.04.091.

9. Y. Chen, X. Zhang, D.C. Dunand, C.A. Schuh, Y. Chen, X. Zhang, D.C. Dunand, C.A. Schuh, Shape memory and superelasticity in polycrystalline Cu – Al – Ni microwires Shape memory and superelasticity in polycrystalline Cu – Al – Ni microwires, 2017 , 171906 ,17–20, doi:10.1063/1.3257372.
10. K. Akash, A.K. Shukla, S.S. Mani Prabu, D.C. Narayane, S. Kanmanisubbu, I.A. Palani, Parametric investigations to enhance the thermomechanical properties of CuAlNi shape memory alloy Bi-morph, J. Alloys Compd. 2017, 720 , 264–271. doi:10.1016/j.jallcom.2017.05.255.
11. K. Akash, S.S. Mani Prabu, T. Gustmann, S. Jayachandran, S. Pauly, I.A. Palani, Enhancing the life cycle behaviour of Cu-Al-Ni shape memory alloy bimorph by Mn addition, Mater. Lett. 2018 ,226 , 55–58. doi:10.1016/j.matlet.2018.05.008.
12. A. V Shelyakov, A.Y. Terekhov, Fiber-Optic Thermosensor Based on Shape Memory Effect, 1995 , 5 , 1183–1186.
13. J.A. Balta, F. Bosia, V. Michaud, G. Dunkel, J. Botsis, J.A. Manson, Smart composites with embedded shape memory alloy actuators and fiber Bragg grating sensors: Activation and control, Smart Mater. Struct. , 2005 , 14 , 457–465. doi:10.1088/0964-1726/14/4/001.
14. K.P. Mohanchandra, S. Karnani, M.C. Emmons, W.L. Richards, G.P. Carman, Thin film NiTi coatings on optical fiber Bragg sensors, Appl. Phys. Lett. 2008, 93. doi:10.1063/1.2961002.
15. K.P. Mohanchadra, M.C. Emmons, S. Karnani, G.P. Carman, W.L. Richards, Asme, Response of Optical Fiber Bragg Sensors With a Thin Film Shape Memory Alloy Coating, Smasis2008 Proc. Asme Conf. Smart Mater. Adapt. Struct. Intell. Syst. - 2008, Vol 1. (2009) 85–89. doi:10.1115/SMASIS2008-455.
16. A. K., C. K., P. G., N. Dhiraj C., R. Disawal, B.K. Lad, V. Singh, P. I. A., Investigations on transformer oil temperature sensing using CuAlNi/polyimide shape memory alloy composite film , 2017, 10165 , 101651C. doi:10.1117/12.2259898.
17. S.N. Saud, E. Hamzah, T. Abubakar, R.H. S, Jurnal Teknologi Full paper

A Review on Influence of Alloying Elements on the Microstructure and Mechanical Properties of Cu-Al-Ni Shape Memory Alloys, J. Teknol.2013, 1 51–56.

18. C.A. Canbay, Z. Karagoz, Effects of Annealing Temperature on Thermomechanical Properties of Cu-Al-Ni Shape Memory Alloys, Int. J. Thermophys. 2013, 34 ,1325–1335. doi:10.1007/s10765-013-1486-z.
19. T. Mineta, K. Kasai, Y. Sasaki, E. Makino, T. Kawashima, T. Shibata, Microelectronic Engineering Flash-evaporated TiNiCu thick film for shape memory alloy micro actuator Substrate Shutter Guide pipe, Microelectron. Eng.2009, 86 ,1274–1277. doi:10.1016/j.mee.2008.12.032.
20. G.H. Chandra, J.N. Kumar, N.M. Rao, S. Uthanna, Preparation and characterization of flash evaporated tin selenide thin films, Journal of Crystal Growth ,2007, 306 , 68–74. doi:10.1016/j.jcrysgro.2007.05.004.
21. W. Huang, On the selection of shape memory alloys for actuators, Mater. Des. 2002,23 ,11–19. doi:10.1016/S0261-3069(01)00039-5.
22. Abdi, O., Kowalsky, M., Hassan, T., Kiesel, S., & Peters, K. (2008, April). Large deformation polymer optical fiber sensors for civil Infrastructure systems. In Sensors and Smart Structures Technologies for Civil, Mechanical, and Aerospace Systems 2008 , 6932, 693242). International Society for Optics and Photonics.
23. J. Huang, D. Křemenáková, J. Militký, G. Zhu, Y. Wang, Evaluation of illumination intensity of plastic optical fibers with tio2 particles by laser treatment, Autex Res. J. 2015,15 , 13–18. doi:10.2478/aut-2014-0016.
24. Rointan F. Bunshah , [Hand Book of Hard Coatings Deposition Technologies,Properties and Applications], Journal of Visual Languages & Computing 2002, 0815514387.
25. M. Ennuyer, Evolution des suivis d'élevage, Synthesis and characterization of Cu–Al–Ni shape memory alloy multilayer thin films, Journal of Thin Solid Films , 1999 , Point Vet. 30 711–716. doi:10.1016/j.tsf.2012.12.062.
26. B. Sutapun, M. Tabib-azar, M.A. Huff, Applications of shape memory alloys in optics, 37 (1998) 6811–6815.

27. Huang, X. and Liu, Y., 2005. Surface morphology of sputtered NiTi-based shape memory alloy thin films. *Surface and Coatings Technology*, *190*(2), pp.400-405.
28. Fu, Y.Q., Luo, J.K., Flewitt, A.J., Huang, W.M., Zhang, S., Du, H.J. and Milne, W.I., 2009. Thin film shape memory alloys and microactuators. *International Journal of Computational Materials Science and Surface Engineering*, *2*(3-4), pp.208-226.
29. Crozier, K.B., Yaralioglu, G.G., Degertekin, F.L., Adams, J.D., Minne, S.C. and Quate, C.F., 2000. Thin film characterization by atomic force microscopy at ultrasonic frequencies. *Applied physics letters*, *76*(14), pp.1950-1952.
30. S.K. Vajpai, R.K. Dube, S. Sangal, Microstructure and properties of Cu-Al-Ni shape memory alloy strips prepared via hot densification rolling of argon atomized powder preforms, Mater. Sci. Eng. A. 529 (2011) 378–387. doi:10.1016/j.msea.2011.09.046.
31. A.K. Tiwari, V.K. Verma, T. a. Jain, P.K. Bajpai, Conclusive Growth of CdTe Nanorods by Solvothermal Decomposition Using Single Source Precursors, Soft Nanosci. Lett. 2013, 03 , 52–57. doi:10.4236/snl.2013.33010.
32. X. Liu, H. Du, P. Wang, T.T. Lim, X.W. Sun, A high-performance UV/visible photodetector of Cu2O/ZnO hybrid nanofilms on SWNT-based flexible conducting substrates, J. Mater. Chem. C. 2014 , 2 ,9536–9542. doi:10.1039/c4tc01585a.
33. V. Sampath, Studies on the effect of grain refinement and thermal processing on shape memory characteristics of Cu-Al-Ni alloys, Smart Mater. Struct. 14 (2005). doi:10.1088/0964-1726/14/5/013.
34. K. Akash, A.K. Jain, G. Karmarkar, A. Jadhav, D.C. Narayane, N. Patra, I.A. Palani, Investigations on actuation characteristics and life cycle behaviour of CuAlNiMn shape memory alloy bimorph towards flappers for aerial robots, Mater. Des. 2018,144 , 64–71. doi:10.1016/j.matdes.2018.02.013.
35. J. Loskyll, W.F. Maier, K. Stoewe, Application of a simultaneous TGA-DSC thermal analysis system for high-throughput screening of catalytic

activity, ACS Comb. Sci., 2012 , 14 600–604. doi:10.1021/co3000659.

36. P.L. Potapov, E.P. Da Silva, Time response of shape memory alloy actuators, J. Intell. Mater. Syst. Struct. 11 (2000) 125–134. doi:10.1106/XH1H-FH3Q-1YEX-4H3F.
37. R.N. Saunders, J.G. Boyd, D.J. Hartl, J.K. Brown, F.T. Calkins, D.C. Lagoudas, A validated model for induction heating of shape memory alloy actuators, Smart Mater. Struct. 25 (2016) 0. doi:10.1088/0964-1726/25/4/045022.
38. A. K, M.P. S S, A.K. Shukla, T. Nath, K. S, I.A. Palani, Investigations on the life cycle behavior of Cu-Al-Ni/polyimide shape memory alloy bi-morph at varying substrate thickness and actuation conditions, Sensors Actuators, A Phys. 254 (2017) 28–35. doi:10.1016/j.sna.2016.12.008.
39. Li, Z., Pan, Z.Y., Tang, N., Jiang, Y.B., Liu, N., Fang, M. and Zheng, F., Cu–Al–Ni–Mn shape memory alloy processed by mechanical alloying and powder metallurgy, Materials Science and Engineering: A, 2006,417(1-2), pp.225-229.
40. Dimitris C. Lagoudas, Shape Memory Alloys: Modeling and Engineering Applications, Springer, 2008, doi:10.1007/978-0-387-47685-8.
41. Canbay, C. A., & Karagoz, Z. (2013). Effects of annealing temperature on thermomechanical properties of Cu–Al–Ni shape memory alloys , International Journal of Thermophysics ,2013,34(7) , 1325-1335.
42. T.N. Raju, V. Sampath, Effect of Ternary Addition of Iron on Shape Memory Characteristics of Cu-Al Alloys.pdf, 20 (2011) 767–770. doi:10.1007/s11665-011-9916-1.
43. E. Wongweerayoot, W. Srituravanich, A. Pimpin, Fabrication and Characterization of Nitinol-Copper Shape Memory Alloy Bimorph Actuators, J. Mater. Eng. Perform. 24 (2014) 635–643. doi:10.1007/s11665-014-1334-8.
44. K. Malukhin, K. Ehmann, Material Characterization of NiTi Based Memory Alloys Fabricated by the Laser Direct Metal Deposition Process, 128 (2016) 691–696. doi:10.1115/1.2193553.
45. JAMES A. KIDD JR, The Effect of Flexural Strain On The Transmissivity of Optical Fiber, 33 (1991).